

000 001 002 003 004 005 006 007 008 009 010 011 012 013 014 015 016 017 018 019 020 021 022 023 024 025 026 027 028 029 030 031 032 033 034 035 036 037 038 039 040 041 042 043 044 045 046 047 048 049 050 051 052 053 OPTIMAL STOPPING VS BEST-OF- N FOR INFERENCE TIME OPTIMIZATION

Anonymous authors

Paper under double-blind review

ABSTRACT

Large language model (LLM) generation often requires balancing output quality against inference cost, especially when using multiple generations. We introduce a new framework for inference-time optimization based on the classical Pandora’s Box problem. Viewing each generation as opening a costly “box” with random reward, we develop algorithms that decide when to stop generating without knowing the underlying reward distribution. Our first contribution is a UCB-style Pandora’s Box algorithm, which achieves performance that is provably close Weitzman’s algorithm, the optimal strategy when the distribution is known. We further adapt this method to practical LLM settings by addressing reward scaling across prompts via a Bradley–Terry inspired transformation. This leads to an adaptive inference-time optimization method that normalizes rewards and learns stopping thresholds on the fly. Experiments on the AlpacaFarm and HH-RLHF datasets, using multiple LLM–reward model pairs, show that our adaptive strategy can obtain the same performance as non-adaptive Best-of- N sampling while requiring 15–35% fewer generations on average. Our results establish a principled bridge between optimal stopping theory and inference-time scaling, providing both theoretical performance bounds and practical efficiency gains for LLM deployment.

1 INTRODUCTION

Large language models (LLMs) are increasingly deployed in applications where both quality and efficiency are critical (Achiam et al., 2023; Hoffmann et al., 2022). A widely used approach to improve generation quality is Best-of- N sampling: generate N candidate responses, score them with a reward model, and select the best (Nakano et al., 2021; Touvron et al., 2023). While effective, this approach wastes compute: the number of generations is fixed in advance, even if an acceptable output is found early or if a prompt is inherently easy (Wang et al., 2025; Sun et al., 2024; Manvi et al., 2024). As models scale and inference costs rise, the need for adaptive inference-time strategies that dynamically balance quality and compute has become urgent (Snell et al., 2025; Jin et al., 2025).

Several recent methods have sought to improve inference-time efficiency. Reranking strategies (e.g., Best-of- N , rejection sampling, majority-vote) improve quality but rely on over-generation, making them computationally expensive (Wang et al., 2025; Manvi et al., 2024; Jain et al., 2023; Wang et al., 2022). Speculative decoding accelerates sampling by offloading work to a smaller draft model, but it does not address how many generations to produce (Leviathan et al., 2023; Chen et al., 2023). Early stopping heuristics exist in practice, yet they lack theoretical guarantees and often underperform on difficult prompts (Agrawal et al., 2024; He et al., 2025; Wei et al., 2025). Overall, there lacks a principled framework for deciding when to stop generating while maintaining near-optimal reward.

In this paper, we introduce a new perspective by connecting LLM inference with the classical Pandora’s Box problem from optimal stopping theory (Weitzman, 1978). In our view, each generation corresponds to opening a costly “box” that yields a random reward. The task is to decide whether to stop and accept the best reward so far or continue generating, *without knowing the underlying reward distribution*. This abstraction provides a rigorous foundation for inference-time optimization, subsuming heuristics like Best-of- N as special cases.

Our Contributions. We develop both theoretical and practical foundations for adaptive LLM inference on the following three fronts:

1. **A UCB-style Pandora’s Box algorithm.** We propose the first stopping strategy that adapts to unknown reward distributions. By maintaining anytime-valid confidence bounds on the optimal stopping threshold, our algorithm guarantees vanishing regret relative to Weitzman’s optimal policy, which assumes full distributional knowledge.¹
2. **A practical adaptive meta-generation framework.** To handle cross-prompt reward scaling issues, we introduce a Bradley–Terry inspired transformation that normalizes rewards. This yields a general-purpose meta-generation procedure that dynamically learns stopping thresholds.
3. **Empirical validation.** On the AlpacaFarm and HH-RLHF dataset, across multiple LLM–reward model pairs, our adaptive strategy achieves the same reward as non-adaptive Best-of- N sampling while requiring 15–35% fewer generations on average. This establishes that principled stopping rules yield concrete efficiency gains in realistic settings.

1.1 RELATED WORKS

Inference-Time Optimization. A growing body of work studies how to allocate inference-time compute more effectively. Beyond Best-of- N , (Nakano et al., 2021; Touvron et al., 2023; Wang et al., 2025; Sun et al., 2024; Manvi et al., 2024), recent methods frame test-time scaling as adaptive self-calibration (Huang et al., 2025; Qu et al., 2025). Chain-of-thought prompting and self-consistency (Wei et al., 2022; Wang et al., 2022) also improve reliability by generating multiple reasoning paths, though at the cost of substantial extra compute. Lastly, Snell et al. (2025) show that prompt-adaptive compute allocation can outperform model scaling, while Jin et al. (2025) analyze energy-accuracy tradeoffs. See the survey by Welleck et al. (2024) for a comprehensive review.

Early Stopping, Confidence, and Adaptive Decoding. Several works address the question of *when to stop* allocating further computation. Classic approaches include adaptive computation time (Graves, 2016) and confident adaptive decoding (Schuster et al., 2022). Agrawal et al. (2024) propose an entropy-based stopping rule during speculative decoding, adaptively halting draft expansion when confidence is sufficient. He et al. (2025) introduce an uncertainty-guided mechanism for code generation, pausing and reranking when uncertainty is high. Similarly, Wei et al. (2025) leverage adaptive layerwise exits to accelerate decoding without sacrificing accuracy. These approaches share our motivation of minimizing unnecessary compute while preserving output quality.

Pandora’s Box and Optimal Stopping. Our approach draws inspiration from the *Pandora’s Box problem*, a classic framework in optimal stopping (Weitzman, 1978). Recent advances have expanded this framework into online and learning-theoretic domains Esfandiari et al. (2019); Gergatsouli & Tzamos (2022); Atsidakou et al. (2024), establishing important connections with prophet inequalities and multi-armed bandit formulations (Gatmiry et al., 2024; Xie et al., 2024). While this problem has generated substantial theoretical insights across various domains, its application to LLM inference remains unexplored. Our work brings this perspective to test-time optimization by framing candidate generation as opening costly boxes.

We review other related works in Appendix B.

2 PRELIMINARIES

2.1 NOTATION

Let \mathcal{X} denote the space of prompts and \mathcal{Y} be the space of responses. A Large Language Model (LLM) $\pi : \mathcal{X} \rightarrow \Delta \mathcal{Y}$ maps a prompt to a distribution over responses, where we let $\Delta \mathcal{Y}$ denote the set of all distributions on \mathcal{Y} . A reward model is a function $r : \mathcal{X} \times \mathcal{Y} \rightarrow \mathbb{R}$ that maps a prompt and a response to a real-value. Given a prompt $x \in \mathcal{X}$, LLM π , and reward model r , we use $D_{r, \pi(x)}$ to denote the distribution over rewards induced by passing x to π , sampling $y \sim \pi(x)$, and then computing $r(x, y)$. We will often just use D as shorthand and use F to denote its CDF and f to denote its PDF, omitting dependence on π , x and r when those are clear from context.

¹We note, however, that Weitzman's algorithm applies to multiple box types. Our results are concerned with the i.i.d. special case, though we expect effective the natural generalization of our approach to multiple boxes will apply to generation from LLM ensembles.

108
1092.2 TEST-TIME STEERING AND BEST-OF- N SAMPLING110
111
112
113
114

After the pre-training stage, the focus often shifts from learning general language ability to steering a model’s outputs toward more desirable responses. One way to formalize this is through a reward model $r : \mathcal{X} \times \mathcal{Y} \rightarrow \mathbb{R}$, which assigns higher scores to responses y for a given prompt x when they exhibit preferred properties. The objective is then to generate outputs that achieve high reward under r at test time. There are two broad ways to influence the outputs of a pre-trained model:

115
116
117

(i) Fine-tuning. Techniques such as reinforcement learning from human feedback (RLHF) fine-tune the model so that high-reward responses are more likely (Christiano et al., 2017; Ouyang et al., 2022).

118
119
120
121

(ii) Test-time steering. Instead of additional training, these methods rely purely on how inference is conducted. Test-time steering treats compute at generation time as the resource to be allocated, biasing outputs toward higher-reward responses by modifying the decoding process (Welleck et al., 2024).

122
123
124
125
126
127
128
129
130
131

A simple and widely studied test-time approach is Best-of- N sampling (Nakano et al., 2021; Tournon et al., 2023). For a given prompt x , we generate N candidate responses $y_1, \dots, y_N \sim \pi(x)$, evaluate each with $r(x, y_i)$, and select the response with the highest score. Best-of- N has been shown to substantially improve output quality across tasks, both empirically and theoretically, (Wang et al., 2025; Sun et al., 2024; Beirami et al., 2024; Yang et al., 2024), but it can be computationally expensive since it requires N forward passes per prompt, with N fixed in advance. Moreover, in practice, N is typically fixed. However, some prompts may yield strong candidates after only a few samples, while others require more, making a uniform budget potentially wasteful. This motivates the design of adaptive test-time strategies that allocate compute more efficiently across prompts.

132
133
134
135
136
137
138

2.3 OPTIMAL STOPPING, PANDORA’S BOX, AND WEITZMAN’S ALGORITHM

The Pandora’s Box problem (Weitzman, 1978) is a classical optimal stopping problem: a decision-maker faces k boxes, each box $i \in [k]$ containing a reward drawn from a known distribution D_i and requiring an opening cost $c_i > 0$. The objective is to adaptively decide which boxes to open and when to stop, maximizing the best observed reward minus total costs. Once opened, a box’s reward can be claimed at any time.

139
140
141
142
143

This framework maps naturally to LLM generation. For a prompt x , an LLM π samples responses from $\pi(x)$, with rewards assigned by a deterministic model r , inducing a reward distribution $D_{r, \pi(x)}$. Each generation incurs a computational cost c that depends on the prompt, model, and reward function. Thus, generating responses mirrors opening boxes: each sample reveals a reward at cost c , and the decision-maker must trade off computation against reward.

144
145
146

A particularly relevant special case is when all boxes share the same distribution D and cost c , modeling repeated queries to a single LLM. We focus on this setting throughout, though extensions to multiple LLMs are natural directions for future work.

147
148

A fundamental concept in solving this problem is the fair-cap value, the threshold where expected excess reward exactly covers the opening cost.

149
150
151
152

Definition 1 (Fair-cap value). *Let D be a distribution and $c > 0$ be the cost value for each sample. The fair-cap value $\tau \in \mathbb{R}$ associated with (D, c) , denoted $\tau(D, c)$, is the number satisfying the equality $\mathbb{E}_{v \sim D} [[v - \tau]_+] = c$, where $[\cdot]_+ = \max(0, \cdot)$.*

153
154
155
156
157

Weitzman’s celebrated algorithm provides the optimal stopping strategy using fair-cap values when distributions are known. Though Weitzman’s algorithm is defined for an arbitrary collection of not-necessarily-identical distributions in general, we describe its special case for infinitely-many boxes with identical distributions below. This corresponds to our focus on a single LLM which can be queried an unbounded number of times.

158
159
160
161

Definition 2 (Weitzman’s Algorithm for infinitely-many identical boxes). *Let D be a known distribution, $c > 0$ be the cost value for each sample, and $\tau := \tau(D, c)$ be the fair-cap value. The algorithm samples from D until it observes a report exceeding τ . More formally: Letting $v_1, v_2, \dots \sim D^\infty$ be a countably infinite sequence of i.i.d. rewards, the stopping time of Weitzman’s algorithm is the random variable $T_W := \inf\{n \geq 1 : \max_{i \leq n} v_i \geq \tau\}$.*

162 In practice, reward distributions are effectively unknown. While implicitly encoded in the model
 163 weights, they lack compact representation and are only accessible through sampling. The meta-
 164 generation problem thus becomes a Pandora’s Box problem with an *unknown* single distribution but
 165 known cost value. To evaluate algorithms in the *unknown* distribution setting, we compare against
 166 an oracle that knows the true distribution and executes Weitzman’s algorithm optimally.

167 **Definition 3** (Additive Sub-optimality Gap). *Consider distribution D with cost c . Let W denote
 168 Weitzman’s optimal policy with full knowledge of D , achieving net payoff R_W (maximum reward
 169 minus total costs). For any policy S that learns D only through sampling, with payoff R_S , the
 170 additive sub-optimality gap is $\mathbb{E}_D[R_W - R_S]$.*

171 In general, if the reward distribution is allowed to be picked completely adversarially, then there is
 172 no hope for designing a single, minimax optimal stopping policy S whose additive sub-optimality
 173 gap is uniformly bounded across all distributions. As a result, we will assume that we have a *known*
 174 distribution family \mathcal{F} such that the *unknown* $D \in \mathcal{F}$.

3 PANDORA’S BOX WITH UNKNOWN REWARD DISTRIBUTIONS

179 When the distribution D is unknown, the fair-cap value τ must be learned from data. Our main
 180 algorithm, *UCB Pandora’s Box*, adapts the upper confidence bound (UCB) principle from multi-
 181 armed-bandit theory (Auer et al., 2002). The algorithm iteratively samples rewards and uses them
 182 along with the family \mathcal{F} to construct an upper confidence bound τ^+ on the fair-cap value τ . It stops
 183 once the maximum observed reward M exceeds the UCB on τ . Pseudo-code is given in Algorithm 2.

184 The specific update for the UCB τ^+ depends on \mathcal{F} and the method for constructing confidence
 185 bounds for τ . In particular, \mathcal{F} must be “nice” enough to admit an *anytime-valid confidence sequence*
 186 for τ . We define this rigorously and provide one such example in Section 3.1. In practice, the
 187 confidence parameter is a hyperparameter that influences the exploration-exploitation balance.

3.1 MAIN THEORETICAL RESULT

190 As previously highlighted, UCB Pandora’s Box requires an anytime-valid upper confidence bound
 191 on the fair-cap value τ . Definition 4 makes this precise.

192 **Definition 4** (Anytime Valid Upper Confidence Bound on the Fair-cap Value). *Let \mathcal{F} be a family of
 193 distributions and $c > 0$ be the cost value for each sample. A function $\tau^+ : \mathbb{N} \times (0, 1) \times \mathbb{R}^* \rightarrow \mathbb{R}$ is
 194 an anytime valid upper confidence bound of the fair-cap value with width function $\sigma : \mathbb{N} \times (0, 1) \times \mathbb{R}$
 195 for \mathcal{F} if for every $\delta \in (0, 1)$ and $D \in \mathcal{F}$, we have*

$$197 \mathbb{P}_{v_{1:\infty} \sim D^\infty} [\forall n \in \mathbb{N} : \tau \in [\tau_\delta^+(n, v_{1:n}) - \sigma_{\delta, \tau}(n), \tau_\delta^+(n, v_{1:n})]] \geq 1 - \delta.$$

198 where $\tau = \tau(D, c)$ is the fair-cap value.

200 If \mathcal{F} is a parametric family of distributions, the fair-cap value often admits a simple monotonic de-
 201 pendence on the distribution’s parameters. This observation allows us to obtain an upper confidence
 202 bound on the fair-cap value by applying the same monotonic transformation to an upper confidence
 203 bound on the parameters themselves. For example, in Section 6 we show that when \mathcal{F} is the class
 204 of Exponential distributions, an upper confidence bound on the mean directly yields an upper con-
 205 fidence bound on the fair-cap value. More generally, constructing a confidence sequence for τ can
 206 be reduced to two steps: (1) build a confidence sequence for the distribution’s parameters, and (2)
 207 propagate it through the monotonic mapping to obtain a confidence sequence for the fair-cap value.

208 We now present Theorem 5, our main theoretical result of this section, which upper bounds the
 209 additive sub-optimality gap of UCB Pandora’s Box algorithm.

210 **Theorem 5** (Upper bound on Additive Sub-optimality). *Let \mathcal{F} be a family of distributions and $c > 0$
 211 be the cost value for each sample. Let $\tau_\delta^+(n, v_{1:n})$ be an anytime upper confidence bound with
 212 deterministic width $\sigma_{\delta, \tau}(n)$ for \mathcal{F} according to Definition 4. i.e., for every distribution $D \in \mathcal{F}$, on
 213 the event $E_\delta := \left\{ \forall n \geq 1 : \tau \leq \tau_\delta^+(n, v_{1:n}) \leq \tau + \sigma_{\delta, \tau}(n) \right\}$ we have that $\mathbb{P}_{v_1, v_2, \dots \sim D}(E_\delta) \geq 1 - \delta$.
 214 Consider the two stopping policies:*

- **Weitzman policy:** $T_W := \inf\{n \geq 1 : \max_{i \leq n} v_i \geq \tau\}$ w/ $R_W := \max_{i \leq T_W} v_i - c T_W$.

216 • **UCB policy:** $T_U := \inf\{n \geq 1 : \max_{i \leq n} v_i \geq \tau_\delta^+(n, v_{1:n})\}$ w/ $R_U := \max_{i \leq T_U} v_i - c T_U$.
 217

218 Then for every $D \in \mathcal{F}$ and $\delta \in (0, 1)$, we have that
 219

220
$$\mathbb{E}_D [(R_W - R_U) \mathbf{1}_{E_\delta}] \leq \sum_{n=1}^{\infty} \sigma_{\delta, \tau}(n) (1 - F_D(\tau)) \left(F_D^{n-1}(\tau + \sigma_{\delta, \tau}(n)) - F_D^{n-1}(\tau) \right),$$

 221

222 where F_D is the CDF of D and $\tau = \tau(D, c)$ is the fair-cap value of D .
 223

224 The proof of Theorem 5 can be found in Appendix E.
 225

226 3.2 EXAMPLE: EXPONENTIAL DISTRIBUTION WITH UNKNOWN PARAMETER λ
 227

228 The upper bound in Theorem 5 is abstract and instance-dependent. To obtain a more concrete result,
 229 we instantiate it with the family \mathcal{F} of Exponential distributions parametrized by $\lambda \in (0, 1/(ce)]$.
 230

231 For λ in this range, let $D_\lambda \in \mathcal{F}$ denote the Exponential distribution with rate λ , with CDF $F_\lambda(x) =$
 232 $1 - e^{-\lambda x}$ and PDF $f_\lambda(x) = \lambda e^{-\lambda x}$. The restriction $\frac{1}{\lambda} \geq ec$ ensures that the sampling cost c is at
 233 most $1/e$ of the expected reward. Indeed, if $c > 1/\lambda$, not even a single sample would be worthwhile.

234 Theorem 6 provides an any-time valid UCB on the fair-cap value for distributions in \mathcal{F} .
 235

236 **Theorem 6** (Anytime-valid Upper Confidence Bound for Exponential Fair-cap value). *Let $c > 0$ be
 237 the sampling cost and \mathcal{F} be the class of Exponential distributions with parameter $\lambda \in (0, \frac{1}{ce}]$. Then,
 238 the function $\tau_\delta^+(n, v_{1:n}) = \hat{\mu}_n(1 + r_\delta(n)) \log\left(\frac{\hat{\mu}_n(1 + r_\delta(n))}{c}\right)$ with width function $\sigma_{\delta, \tau}(n) = 16\tau$ ·
 239 $r_\delta(n)$ is an anytime valid upper confidence bound on the fair-cap value, where $\hat{\mu}_n = \frac{1}{n} \sum_{i=1}^n v_i$,
 240 and $r_\delta(n) := \min\left\{\frac{1}{2}, \sqrt{\frac{6}{n} \log\left(\frac{2n(n+1)}{\delta}\right)}\right\}$.*
 241

242 The proof of Theorem 6 (Appendix E.2) proceeds by expressing the fair-cap value of an Exponential
 243 distribution as a monotonic function of its mean, constructing an anytime-valid UCB for the mean,
 244 and then transferring this bound to the fair-cap value. With Theorem 6 in hand, we can now explicitly
 245 compute the right-hand side of the expected sub-optimality gap in Theorem 5.

246 **Corollary 7** (Sub-optimality gap upper bound for Exponential distribution). *Let $c > 0$ be the sam-
 247 pling cost and \mathcal{F} be the class of Exponential distribution with parameter $\lambda \in (0, \frac{1}{ce}]$. Then, for
 248 every $\delta \in (0, 1)$ and $D_\lambda \in \mathcal{F}$ we have that*
 249

250
$$\sum_{n=1}^{\infty} \sigma_{\delta, \tau}(n) \cdot (1 - F_\lambda(\tau)) \cdot (F_\lambda^{n-1}(\tau + \sigma_{\delta, \tau}(n)) - F_\lambda^{n-1}(\tau)) \leq \tilde{O}_\delta\left(\frac{1}{\lambda}\right),$$

 251

252 where $\sigma_{\delta, \tau}(n)$ is defined as in Theorem 6, $\tau = \tau(D_\lambda, c)$ is the fair-cap value, and $\tilde{O}_\delta(\cdot)$ hides
 253 polylog terms of $\frac{1}{\delta}$. As a result, we have that for every $\delta \in (0, 1)$ and $D_\lambda \in \mathcal{F}$ the additive sub-
 254 optimality gap for UCB Pandora’s Algorithm satisfies $\mathbb{E}_{D_\lambda} [(R_W - R_U) \mathbf{1}_{E_\delta}] \leq \tilde{O}_\delta\left(\frac{1}{\lambda}\right)$.
 255

256 At a high level, Corollary 7 (proved in Appendix E.2) shows that under event E_δ (see Theorem 5), the
 257 expected sub-optimality gap of UCB Pandora’s Box is bounded by the mean $1/\lambda$ (up to logarithmic
 258 factors in δ). In Section 4, we leverage these results to develop prompt-adaptive inference-time
 259 optimization methods.
 260

261 4 APPLYING UCB PANDORA’S BOX TO INFERENCE-TIME OPTIMIZATION
 262

263 Building on the connection between test-time steering and the Pandora’s Box problem established in
 264 Section 2.3, we now cast inference-time optimization as an instance of the Pandora’s Box problem.
 265 Each generation from the base LLM can be viewed as opening a costly box whose payoff is the
 266 reward assigned by r . The challenge is to decide when to stop sampling: too early risks missing high-
 267 reward outputs, while too late wastes computation. In what follows, we develop adaptive stopping
 268 rules that navigate this tradeoff without prior knowledge of the underlying reward distribution.
 269

270 4.1 THE REWARD SCALING CHALLENGE
271

272 A key subtlety in framing inference-time optimization as a Pandora’s Box problem is deciding what
273 makes a response “high quality.” Using a fixed reward threshold is inadequate because reward scales
274 vary dramatically across prompts. For example, Figure 4 in Appendix D shows large variance in
275 median rewards across 100 prompts, even when evaluated with the same model.

276 To enable cost-shared semantics across prompts with different reward scales, we adopt a percentile-
277 based approach. Specifically, we select a gold standard percentile α of the reward distribution as our
278 quality benchmark. This choice naturally adapts to each prompt’s reward scale while maintaining
279 consistent quality standards. Throughout our work, we set $\alpha = 0.99$ to compete with best-of- N
280 sampling (where typically $\alpha \approx 1 - \frac{1}{N}$), though practitioners may adjust this parameter based on
281 quality requirements. We formalize this approach through what we term the “acceptance criterion”:

282 **Definition 8** (Acceptance Criterion). *A response $y \in \mathcal{Y}$ to prompt $x \in \mathcal{X}$ is acceptable with respect
283 to the LM-reward model pair (π, r) if its reward $r(x, y)$ exceeds the α -percentile of the reward
284 distribution $D_{r, \pi(x)}$, denoted $D_{r, \pi(x)}^\alpha$. We set $\alpha = 99$ throughout, though larger values correspond
285 to stricter acceptance.*

286 Even so, scaling issues remain. For two prompts x_1 and x_2 , the 99th percentiles $D_{r, \pi(x_1)}^\alpha$ and
287 $D_{r, \pi(x_2)}^\alpha$ may differ greatly (e.g., $D_{r, \pi(x_1)}^\alpha \ll D_{r, \pi(x_2)}^\alpha$), yet exceeding either yields the same utility
288 B . This mismatch between reward magnitude and utility motivates the need for *normalization*.

290 4.2 BRADLEY-TERRY TRANSFORMATION FOR REWARD NORMALIZATION
291

292 We resolve the scaling issue through a transformation inspired by the Bradley–Terry model, which
293 also underlies RLHF training (Bradley & Terry, 1952; Christiano et al., 2017). In RLHF, the prob-
294 ability of preferring response A over B is modeled as $\frac{e^{r_A}}{e^{r_A} + e^{r_B}}$, where r_A and r_B are their rewards.
295 We adapt this idea by comparing each response against an acceptance threshold.

296 **Definition 9** (Acceptance Rate). *The acceptance rate of a response y with reward $v_y = r(x, y)$ with
297 respect to threshold κ is defined as $\text{AR}_\kappa(v) = \min \left\{ 2 \cdot \frac{e^v}{e^v + e^\kappa}, 1 \right\}$.*

300 This transformation maps rewards into $[0, 1]$. The Bradley–Terry term $\frac{e^v}{e^v + e^\kappa}$ represents the prob-
301 ability of preferring a response with reward v over one with reward κ . Intuitively, the acceptance
302 rate approximates the probability that an end-user accepts the response: below-threshold responses
303 are accepted in proportion to their quality relative to κ , while at- or above-threshold responses are
304 accepted with certainty. This normalization enables consistent comparisons across prompts with
305 different reward scales. In our application, we set $\kappa = D_{r, \pi(x)}^\alpha$ as in Definition 8, making accep-
306 tance rates prompt-, model-, and reward-dependent. However, as the true distribution is unknown,
307 we estimate $D_{r, \pi(x)}^\alpha$ from samples, which proves sufficiently accurate.

308 The acceptance rate naturally induces a utility function.

309 **Definition 10** (Utility Function). *For an acceptance threshold κ , the utility function $u_\kappa : \mathbb{R} \rightarrow [0, B]$
310 maps rewards to utilities via $u_\kappa(v) = B \cdot \text{AR}_\kappa(v)$, where $B > 0$ is the maximum achievable utility.*

312 Here, responses below the threshold map to utilities in $[0, B]$, while acceptable responses map ex-
313 actly to B . When $\kappa = D_{r, \pi(x)}^\alpha$, $\text{AR}_\kappa(v)$ is the probability that a response with reward v is ac-
314 cepted, B is the utility of an accepted response, and hence $u_\kappa(v)$ is the *expected* utility of a response
315 with reward v (assuming rejected responses get no utility). Pushing the reward distribution $D_{r, \pi(x)}$
316 through u_κ yields the utility distribution $U_{\kappa, r, \pi(x)} := u_\kappa(D_{r, \pi(x)})$ supported on $[0, B]$. Setting cost
317 $c \in [0, B]$ then allows direct comparison of generation costs with achievable utilities.

318 4.3 THE ADAPTIVE ALGORITHM
319

321 We are now ready to adapt the UCB Pandora’s Box Algorithm from Section 3.1 to the Best-of- N
322 inference-time optimization setting. Given a prompt $x \in \mathcal{X}$, LLM π , and reward model r , our
323 algorithm sequentially generates responses and adaptively decides when to stop. After collecting a
minimum number of samples, it estimates the reward distribution’s tail. To do so, we exponentiate

324 the rewards and fit a shifted exponential distribution to the right-tail values (those above the median).
 325 From this fit, we construct both upper and lower confidence bounds (UCB/LCB) on the scale of the
 326 exponential distribution. The LCB on the scale is then used to derive a conservative estimate of
 327 the α percentile of the exponentiated rewards, while the UCB is used to bound the tail distribution
 328 itself. This combination yields an upper confidence bound on the fair-cap value of the true utility
 329 distribution. If the utility of the best reward observed so far exceeds this fair cap, the algorithm
 330 terminates; otherwise, it continues sampling. Pseudocode is given in Algorithm 1.

331

332 **Algorithm 1** Adaptive Best-of-N Sampling via UCB Pandora’s Box

333 **Parameters:** Cost c , Max utility B , Minimum samples t , Percentile α , Confidence parameter δ .

334 **Input:** LLM π , reward model r , prompt x

335 1: Initialize: $S = \emptyset$ (observed rewards) and $M = -\infty$ (max reward)

336 2: **while** True **do**

337 3: Generate response $y \sim \pi(x)$ and compute its reward $r_y = r(x, y)$.

338 4: Update $M \leftarrow \max\{M, r_y\}$ and $S \leftarrow S \cup \{r_y\}$.

339 5: **if** $|S| \geq t$ **then**

340 6: **—Right Tail Estimation via Exponential Distribution—**

341 7: Estimate tail shift $\hat{\theta} \leftarrow e^{\text{median}(S)}$ and scale of shifted tail $\hat{\mu} \leftarrow \text{mean}(\{e^r - \theta : r \in S \text{ such that } r > \text{median}(S)\})$.

342 8: Apply upper and lower confidence estimation:

343

$$\mu_{\text{ucb}} \leftarrow \mu \cdot \left(1 + \sqrt{\frac{\log |S| \cdot \log(1/\delta)}{|S|}}\right) \quad \mu_{\text{lcb}} \leftarrow \mu \cdot \left(1 - \sqrt{\frac{\log |S| \cdot \log(1/\delta)}{|S|}}\right).$$

344

345 9: Let $\hat{D}^{\text{ucb}} \leftarrow \text{ShiftedExp}(\theta, \frac{1}{\mu_{\text{ucb}}})$ and $\hat{D}^{\text{lcb}} \leftarrow \text{ShiftedExp}(\theta, \frac{1}{\mu_{\text{lcb}}})$ be shifted exponential

346 distributions with shift parameter θ and scales $\frac{1}{\mu_{\text{ucb}}}$ and $\frac{1}{\mu_{\text{lcb}}}$ respectively.

347 10: **—Utility Transformation and Fair Cap Computation—**

348 11: Let $\hat{D}_{r, \pi(x)}^{\alpha} \leftarrow \log(\text{Percentile}_{\alpha}(\hat{D}^{\text{lcb}}))$ be a LCB estimate of $D_{r, \pi(x)}^{\alpha}$.

349 12: Define utility distribution $\hat{U} \leftarrow u_{\kappa}(\log(\hat{D}^{\text{ucb}}))$ where $\kappa = \hat{D}_{r, \pi(x)}^{\alpha}$.

350 13: Compute fair-cap value τ for (\hat{U}, c) .

351 14: **if** $u_{\kappa}(M) \geq \tau$ **then**

352 15: **break**

353 16: **end if**

354 17: **end if**

355 18: **end while**

356 19: **Return** the response with reward M

361 **Implementation Efficiency.** The algorithm can be implemented with negligible overhead relative
 362 to generation costs. A priority queue maintains the median and tail statistics with $O(\log n)$
 363 updates and $O(1)$ queries, while streaming updates eliminate redundant computation. Key distribu-
 364 tional operations are closed-form. For example, the α -percentile of the shifted exponential distribu-
 365 tion is computed in $O(1)$ time from an analytical formula. Fair-cap computation requires solving
 366 $\mathbb{E}[\max(v - \tau, 0)] = c$ for the threshold τ . We approximate the expectation via a Riemann sum with
 367 ~ 5000 intervals. Empirically, this achieves under 1% relative error. The subroutine executes over
 368 100 times per second², enabling real-time adaptation during generation. In practice, the overhead of
 369 adaptive stopping is negligible as LLM and reward model forward passes dominate runtime.

370 4.4 TARGET ACCEPTANCE RATE VARIANT

371 Algorithm 1 requires specifying the utility B and cost c , which may be difficult to estimate in prac-
 372 tice. To address this, we provide an alternative formulation that instead targets a desired acceptance
 373 rate. Rather than computing the fair-cap value from utility–cost tradeoffs, this variant sets a target
 374 acceptance rate $\tau_{\text{target}} \in [0, 1]$ that encodes the desired quality level relative to the acceptance thresh-
 375 old. For example, $\tau_{\text{target}} = 0.9$ seeks responses nearly as good as acceptable ones, while $\tau_{\text{target}} = 1$

376

377 ²Measured on a single core of an AMD EPYC 7513 32-Core Processor.

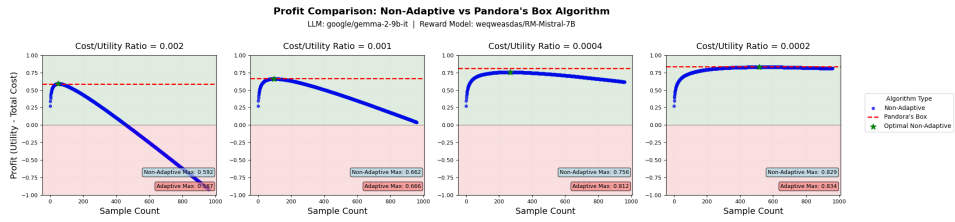


Figure 1: Our algorithm (red) matches optimal non-adaptive performance across varying cost ratios.

requires fully acceptable responses. The algorithm proceeds identically to Algorithm 1 except that the stopping condition is now fixed: it halts when $\text{AR}_{\widehat{D}_{r,\pi(x)}^\alpha}(M) \geq \tau_{\text{target}}^3$. This formulation is useful in settings where quality requirements are clear but utilities are hard to quantify, for instance, when “good enough” responses are well-defined but the value of marginal improvements is ambiguous.

5 EXPERIMENTAL RESULTS

5.1 EXPERIMENTAL SETUP

We evaluate our adaptive Best-of- N algorithm on 100 prompts from AlpacaFarm (Dubois et al., 2023) and 100 from HH-RLHF (Bai et al., 2022). We use four LLM (Google-Gemma-2 (9B), Meta-Llama-3.1 (8B), Mistral-Instruct-v0.3 (7B), Qwen-2.5 (7B)) and two reward models (FsfairX-LLaMA3-RM-v0.1, RM-Mistral-7B; Dong et al., 2023; Xiong et al., 2024). This yields 1,600 generation profiles (2 datasets \times 100 prompts \times 4 LLMs \times 2 reward models). For each profile, we generate 960 responses, compute rewards, and randomize response–reward orderings 100 times to remove ordering effects. We always fix the max utility $B = 1$, and only vary the cost c .

We benchmark against non-adaptive Best-of- N across three tasks: (1) *profit optimization*, comparing utility–cost tradeoffs; (2) *win rate analysis*, under fixed compute budgets; and (3) *efficiency gains*, measuring compute savings at target quality levels. More experimental results are in Appendix F.

5.2 EXPERIMENT 1: PROFIT OPTIMIZATION

We evaluate how well our adaptive algorithm maximizes profit (utility minus total cost) relative to the best non-adaptive strategy. We consider four cost-to-utility ratios: 0.002, 0.001, 0.0004, 0.0002. Figure 1 reports results for Mistral-Instruct-v0.3 (7B) with the RM-Mistral-7B reward model. The adaptive algorithm (red) either closely approximates or outperforms the profit envelope defined by the best non-adaptive strategies (blue/green), automatically achieving this performance without knowing the optimal N in advance. Across all 1,600 generation profiles, the adaptive method outperforms the generator-dependent best non-adaptive algorithm in nearly all cases, demonstrating clear superiority (Figure 5).

5.3 EXPERIMENT 2: WIN RATE UNDER FIXED BUDGET

We compare our adaptive algorithm with non-adaptive Best-of- N under equal computation budgets. For each prompt x , LLM π , and cost $c \in [10^{-5}, 10^{-3}]$, we: (1) run the adaptive algorithm on 100 random orderings and record the average sample count $\bar{n}_{\pi,x,c}$, (2) run non-adaptive Best-of- N with $N = \bar{n}_{\pi,x,c}$ on the same orderings, and (3) compare maximum rewards, awarding half credit for ties. Figure 2 shows the results. The adaptive algorithm consistently outperforms non-adaptive Best-of- N , with win rates exceeding 54% across most cost settings. Gains are largest when costs are low (permitting more samples) or budgets are higher, where adaptive stopping better exploits variation across prompts. Figure 6 confirms these results across different datasets and reward models.

³In this variant, we estimate $\widehat{D}_{r,\pi}^\alpha(x)$ using \widehat{D}^{ucb} . Otherwise, the algorithm tends to stop prematurely by overestimating the acceptance rate of the maximum sample.

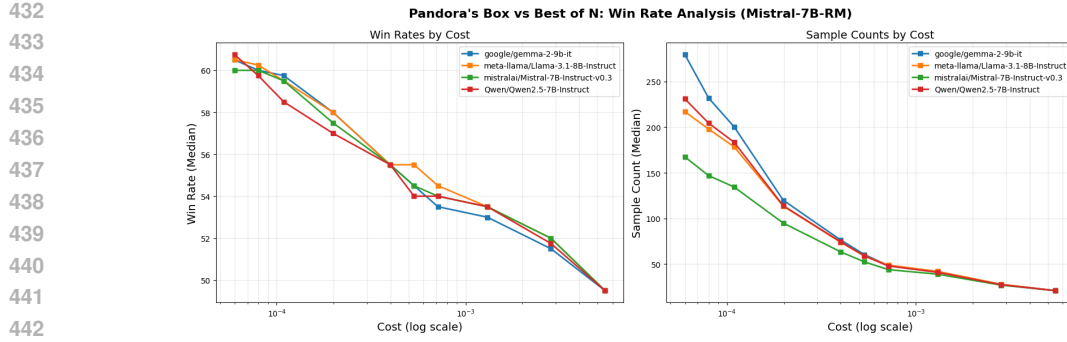


Figure 2: Win rate of the adaptive algorithm compared to non-adaptive Best-of- N . Adaptive stopping leverages computation more effectively, particularly at lower costs.

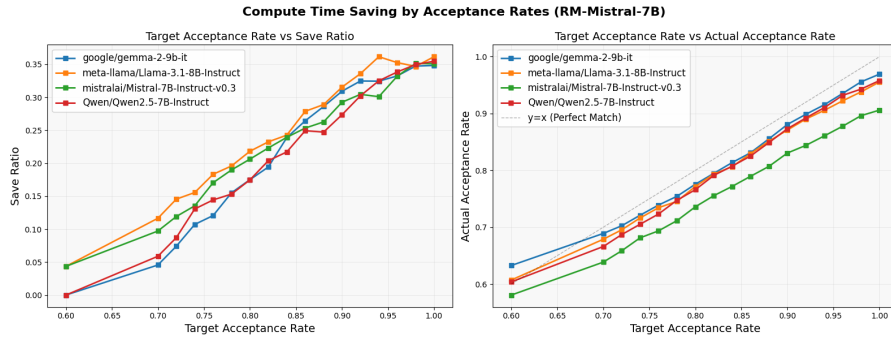


Figure 3: Adaptive algorithm achieves specified target acceptance rates while saving 15–35% of samples compared to non-adaptive Best-of- N .

5.4 EXPERIMENT 3: EFFICIENCY AT TARGET QUALITY LEVELS

We next evaluate the target acceptance rate variant, which allows users to directly specify a desired quality level. For target rates $\tau \in [0.60, 1]$ and each configuration (LLM π , prompt x , target τ), we: (1) measure the adaptive algorithm’s average acceptance rate $\bar{a}_{\pi,x,\tau}$ and sample count $\bar{n}_{\pi,x,\tau}$; (2) identify the non-adaptive N^* that achieves the same $\bar{a}_{\pi,x,\tau}$; and (3) compute the efficiency gain

$$\text{SaveRatio}_{\pi,x,\tau} = \frac{N^* - \bar{n}_{\pi,x,\tau}}{N^*}.$$

Figure 3 shows that the adaptive algorithm both tracks the target quality (right) and yields substantial savings in sample counts (left). For acceptance rates 0.75+, it consistently reduces sampling by 15–35% relative to non-adaptive methods. Savings increase monotonically with stricter targets, from ~15% up to ~35%, reflecting more effective use of learned tail information at higher quality levels.

6 DISCUSSION

We highlight several directions for future investigation. **(1) Multi-model inference:** Although we consider a single LLM in this work, the Pandora’s Box framework extends naturally to ensembles of models, where each model corresponds to a box type with its own cost–quality profile. An open question is whether adaptive algorithms can automatically route queries across models, reducing the need for hand-designed cascades (Yue et al., 2023). **(2) Tree search and reasoning:** Approaches such as tree-of-thought (Yao et al., 2023) and Monte Carlo tree search (Feng et al., 2023) also involve sequential explore–exploit trade-offs at each decision point. Optimal stopping may help formalize when to expand or backtrack in such settings, potentially improving efficiency relative to existing heuristics.

486 REFERENCES
487

488 Josh Achiam, Steven Adler, Sandhini Agarwal, Lama Ahmad, Ilge Akkaya, Florencia Leoni Ale-
489 man, Diogo Almeida, Janko Altenschmidt, Sam Altman, Shyamal Anadkat, et al. Gpt-4 technical
490 report. *arXiv preprint arXiv:2303.08774*, 2023.

491 Sudhanshu Agrawal, Wonseok Jeon, and Mingu Lee. Adaedl: Early draft stopping for specula-
492 tive decoding of large language models via an entropy-based lower bound on token acceptance
493 probability. *arXiv preprint arXiv:2410.18351*, 2024.

494 Alexia Atsidakou, Constantine Caramanis, Evangelia Gergatsouli, Orestis Papadigenopoulos, and
495 Christos Tzamos. Contextual pandora’s box. *Proceedings of the AAAI Conference on Artificial
496 Intelligence*, 38(10):10944–10952, Mar. 2024. doi: 10.1609/aaai.v38i10.28969. URL <https://ojs.aaai.org/index.php/AAAI/article/view/28969>.

497

498 Peter Auer, Nicolo Cesa-Bianchi, and Paul Fischer. Finite-time analysis of the multiarmed bandit
499 problem. *Machine learning*, 47(2):235–256, 2002.

500

501 Yuntao Bai, Andy Jones, Kamal Ndousse, Amanda Askell, Anna Chen, Nova DasSarma, Dawn
502 Drain, Stanislav Fort, Deep Ganguli, Tom Henighan, Nicholas Joseph, Saurav Kadavath, Jack-
503 son Kernion, Tom Conerly, Sheer El Showk, Nelson Elhage, Zac Hatfield-Dodds, Danny Her-
504 nandez, Tristan Hume, Scott Johnston, Shauna Kravec, Liane Lovitt, Neel Nanda, Catherine
505 Olsson, Dario Amodei, Tom B. Brown, Jack Clark, Sam McCandlish, Chris Olah, Benjamin
506 Mann, and Jared Kaplan. Training a helpful and harmless assistant with reinforcement learning
507 from human feedback. *CoRR*, abs/2204.05862, 2022. doi: 10.48550/ARXIV.2204.05862. URL
508 <https://doi.org/10.48550/arXiv.2204.05862>.

509

510 Ahmad Beirami, Alekh Agarwal, Jonathan Berant, Alexander D’Amour, Jacob Eisenstein, Chirag
511 Nagpal, and Ananda Theertha Suresh. Theoretical guarantees on the best-of-n alignment policy.
512 *arXiv preprint arXiv:2401.01879*, 2024.

513 Sujay Bhatt, Ping Li, and Gennady Samorodnitsky. Extreme Bandits using Robust Statistics,
514 September 2021. URL <http://arxiv.org/abs/2109.04433>. arXiv:2109.04433 [stat].

515

516 Ralph Allan Bradley and Milton E Terry. Rank analysis of incomplete block designs: I. the method
517 of paired comparisons. *Biometrika*, 39(3/4):324–345, 1952.

518

519 Boyuan Chen, Mingzhi Zhu, Brendan Dolan-Gavitt, Muhammad Shafique, and Siddharth Garg.
520 Model cascading for code: A cascaded black-box multi-model framework for cost-efficient code
521 completion with self-testing. *arXiv preprint arXiv:2405.15842*, 2024.

522

523 Charlie Chen, Sebastian Borgeaud, Geoffrey Irving, Jean-Baptiste Lespiau, Laurent Sifre, and John
524 Jumper. Accelerating large language model decoding with speculative sampling. *arXiv preprint
arXiv:2302.01318*, 2023.

525

526 Paul F Christiano, Jan Leike, Tom Brown, Miljan Martic, Shane Legg, and Dario Amodei. Deep
527 reinforcement learning from human preferences. *Advances in neural information processing sys-
tems*, 30, 2017.

528

529 Vincent A Cicirello and Stephen F Smith. The Max K-Armed Bandit: A New Model of Exploration
530 Applied to Search Heuristic Selection.

531

532 Hanze Dong, Wei Xiong, Deepanshu Goyal, Rui Pan, Shizhe Diao, Jipeng Zhang, Kashun Shum,
533 and Tong Zhang. Raft: Reward ranked finetuning for generative foundation model alignment.
534 *arXiv preprint arXiv:2304.06767*, 2023.

535

536 Yann Dubois, Xuechen Li, Rohan Taori, Tianyi Zhang, Ishaan Gulrajani, Jimmy Ba, Carlos
537 Guestrin, Percy Liang, and Tatsunori B. Hashimoto. Alpacafarm: A simulation framework for
538 methods that learn from human feedback, 2023.

539 Hossein Esfandiari, Mohammad Taghi Haji Aghayi, Brendan Lucier, and Michael Mitzenmacher.
Online pandora’s boxes and bandits. In *Proceedings of the Thirty-Third AAAI Conference on Artificial
Intelligence and Thirty-First Innovative Applications of Artificial Intelligence*

540 *Conference and Ninth AAAI Symposium on Educational Advances in Artificial Intelligence,*
 541 AAAI'19/IAAI'19/EAII'19. AAAI Press, 2019. ISBN 978-1-57735-809-1. doi: 10.1609/aaai.
 542 v33i01.33011885. URL <https://doi.org/10.1609/aaai.v33i01.33011885>.

543 Xidong Feng, Ziyu Wan, Muning Wen, Stephen Marcus McAleer, Ying Wen, Weinan Zhang, and
 544 Jun Wang. Alphazero-like tree-search can guide large language model decoding and training.
 545 *arXiv preprint arXiv:2309.17179*, 2023.

546 Khashayar Gatmiry, Thomas Kesselheim, Sahil Singla, and Yifan Wang. Bandit algorithms for
 547 prophet inequality and pandora's box. In *SODA*, pp. 462–500, 2024. URL <https://doi.org/10.1137/1.9781611977912.18>.

548 Evangelia Gergatsouli and Christos Tzamos. Online learning for min sum set cover and pandora's
 549 box. In Kamalika Chaudhuri, Stefanie Jegelka, Le Song, Csaba Szepesvari, Gang Niu, and Sivan
 550 Sabato (eds.), *Proceedings of the 39th International Conference on Machine Learning*, volume
 551 162 of *Proceedings of Machine Learning Research*, pp. 7382–7403. PMLR, 17–23 Jul 2022. URL
 552 <https://proceedings.mlr.press/v162/gergatsouli22a.html>.

553 Evangelia Gergatsouli and Christos Tzamos. Online learning for min sum set cover and pandora's
 554 box. In Kamalika Chaudhuri, Stefanie Jegelka, Le Song, Csaba Szepesvari, Gang Niu, and Sivan
 555 Sabato (eds.), *Proceedings of the 39th International Conference on Machine Learning*, volume
 556 162 of *Proceedings of Machine Learning Research*, pp. 7382–7403. PMLR, 17–23 Jul 2022. URL
 557 <https://proceedings.mlr.press/v162/gergatsouli22a.html>.

558 Alex Graves. Adaptive computation time for recurrent neural networks. *arXiv preprint*
 559 *arXiv:1603.08983*, 2016.

560 Kaifeng He, Mingwei Liu, Chong Wang, Zike Li, Yanlin Wang, Xin Peng, and Zibin Zheng.
 561 Adadec: Uncertainty-guided adaptive decoding for llm-based code generation. *arXiv preprint*
 562 *arXiv:2506.08980*, 2025.

563 Jordan Hoffmann, Sebastian Borgeaud, Arthur Mensch, Elena Buchatskaya, Trevor Cai, Eliza
 564 Rutherford, Diego de Las Casas, Lisa Anne Hendricks, Johannes Welbl, Aidan Clark, et al. Training
 565 compute-optimal large language models. *arXiv preprint arXiv:2203.15556*, 2022.

566 Chengsong Huang, Langlin Huang, Jixuan Leng, Jiacheng Liu, and Jiaxin Huang. Efficient Test-
 567 Time Scaling via Self-Calibration, February 2025. URL <http://arxiv.org/abs/2503.00031> [cs].

568 Siddhartha Jain, Xiaofei Ma, Anoop Deoras, and Bing Xiang. Lightweight reranking for language
 569 model generations. *arXiv preprint arXiv:2307.06857*, 2023.

570 Yunho Jin, Gu-Yeon Wei, and David Brooks. The energy cost of reasoning: Analyzing energy usage
 571 in llms with test-time compute. *arXiv preprint arXiv:2505.14733*, 2025.

572 Yaniv Leviathan, Matan Kalman, and Yossi Matias. Fast inference from transformers via speculative
 573 decoding. In *International Conference on Machine Learning*, pp. 19274–19286. PMLR, 2023.

574 Rohin Manvi, Anikait Singh, and Stefano Ermon. Adaptive Inference-Time Compute: LLMs Can
 575 Predict if They Can Do Better, Even Mid-Generation, October 2024. URL <http://arxiv.org/abs/2410.02725> [cs].

576 Alireza Mohammadshahi, Arshad Rafiq Shaikh, and Majid Yazdani. Routoo: Learning to route to
 577 large language models effectively. *arXiv preprint arXiv:2401.13979*, 2024.

578 Reiichiro Nakano, Jacob Hilton, Suchir Balaji, Jeff Wu, Long Ouyang, Christina Kim, Christo-
 579 pher Hesse, Shantanu Jain, Vineet Kosaraju, William Saunders, et al. Webgpt: Browser-assisted
 580 question-answering with human feedback. *arXiv preprint arXiv:2112.09332*, 2021.

581 Long Ouyang, Jeffrey Wu, Xu Jiang, Diogo Almeida, Carroll Wainwright, Pamela Mishkin, Chong
 582 Zhang, Sandhini Agarwal, Katarina Slama, Alex Ray, et al. Training language models to fol-
 583 low instructions with human feedback. *Advances in neural information processing systems*, 35:
 584 27730–27744, 2022.

585 Yuxiao Qu, Matthew Y. R. Yang, Amrith Setlur, Lewis Tunstall, Edward Emanuel Beeching, Ruslan
 586 Salakhutdinov, and Aviral Kumar. Optimizing Test-Time Compute via Meta Reinforcement Fine-
 587 Tuning, March 2025. URL <http://arxiv.org/abs/2503.07572>. arXiv:2503.07572
 588 [cs].

589 Yuxiao Qu, Matthew Y. R. Yang, Amrith Setlur, Lewis Tunstall, Edward Emanuel Beeching, Ruslan
 590 Salakhutdinov, and Aviral Kumar. Optimizing Test-Time Compute via Meta Reinforcement Fine-
 591 Tuning, March 2025. URL <http://arxiv.org/abs/2503.07572>. arXiv:2503.07572
 592 [cs].

593 Yuxiao Qu, Matthew Y. R. Yang, Amrith Setlur, Lewis Tunstall, Edward Emanuel Beeching, Ruslan
 594 Salakhutdinov, and Aviral Kumar. Optimizing Test-Time Compute via Meta Reinforcement Fine-
 595 Tuning, March 2025. URL <http://arxiv.org/abs/2503.07572>. arXiv:2503.07572
 596 [cs].

594 Tal Schuster, Adam Fisch, Jai Gupta, Mostafa Dehghani, Dara Bahri, Vinh Tran, Yi Tay, and Donald
 595 Metzler. Confident adaptive language modeling. *Advances in Neural Information Processing*
 596 *Systems*, 35:17456–17472, 2022.

597 Charlie Victor Snell, Jaehoon Lee, Kelvin Xu, and Aviral Kumar. Scaling llm test-time compute
 598 optimally can be more effective than scaling parameters for reasoning. In *The Thirteenth Inter-*
 599 *national Conference on Learning Representations*, 2025.

600 Matthew J Streeter and Stephen F Smith. An Asymptotically Optimal Algorithm for the Max k-
 601 Armed Bandit Problem.

602 Hanshi Sun, Momin Haider, Ruiqi Zhang, Huitao Yang, Jiahao Qiu, Ming Yin, Mengdi Wang, Peter
 603 Bartlett, and Andrea Zanette. Fast Best-of-N Decoding via Speculative Rejection, October 2024.
 604 URL <http://arxiv.org/abs/2410.20290>. arXiv:2410.20290 [cs].

605 Hugo Touvron, Louis Martin, Kevin Stone, Peter Albert, Amjad Almahairi, Yasmine Babaei, Niko-
 606 lay Bashlykov, Soumya Batra, Prajjwal Bhargava, Shruti Bhosale, et al. Llama 2: Open founda-
 607 tion and fine-tuned chat models. *arXiv preprint arXiv:2307.09288*, 2023.

608 Xuezhi Wang, Jason Wei, Dale Schuurmans, Quoc Le, Ed Chi, Sharan Narang, Aakanksha Chowdh-
 609 ery, and Denny Zhou. Self-consistency improves chain of thought reasoning in language models.
 610 *arXiv preprint arXiv:2203.11171*, 2022.

611 Yiming Wang, Pei Zhang, Siyuan Huang, Baosong Yang, Zhuosheng Zhang, Fei Huang, and Rui
 612 Wang. Sampling-Efficient Test-Time Scaling: Self-Estimating the Best-of-N Sampling in Early
 613 Decoding, March 2025. URL <http://arxiv.org/abs/2503.01422>. arXiv:2503.01422
 614 [cs].

615 Jason Wei, Xuezhi Wang, Dale Schuurmans, Maarten Bosma, Fei Xia, Ed Chi, Quoc V Le, Denny
 616 Zhou, et al. Chain-of-thought prompting elicits reasoning in large language models. *Advances in*
 617 *neural information processing systems*, 35:24824–24837, 2022.

618 Zhepei Wei, Wei-Lin Chen, Xinyu Zhu, and Yu Meng. Adadecode: Accelerating llm decoding with
 619 adaptive layer parallelism. *arXiv preprint arXiv:2506.03700*, 2025.

620 Martin Weitzman. *Optimal search for the best alternative*, volume 78. Department of Energy, 1978.

621 Sean Welleck, Amanda Bertsch, Matthew Finlayson, Hailey Schoelkopf, Alex Xie, Graham Neubig,
 622 Ilia Kulikov, and Zaid Harchaoui. From decoding to meta-generation: Inference-time algorithms
 623 for large language models. *Transactions on Machine Learning Research*, October 2024. URL
 624 <https://arxiv.org/abs/2406.16838>.

625 Qian Xie, Raul Astudillo, Peter I. Frazier, Ziv Scully, and Alexander Terenin. Cost-aware bayesian
 626 optimization via the pandora’s box gittins index. In *The Thirty-eighth Annual Conference on*
 627 *Neural Information Processing Systems*, 2024. URL [https://openreview.net/forum?](https://openreview.net/forum?id=Ouc1F0Sfb7)
 628 [id=Ouc1F0Sfb7](https://openreview.net/forum?id=Ouc1F0Sfb7).

629 Wei Xiong, Hanze Dong, Chenlu Ye, Ziqi Wang, Han Zhong, Heng Ji, Nan Jiang, and Tong Zhang.
 630 Iterative preference learning from human feedback: Bridging theory and practice for rlhf under
 631 kl-constraint, 2024.

632 Joy Qiping Yang, Salman Salamatian, Ziteng Sun, Ananda Theertha Suresh, and Ahmad Beirami.
 633 Asymptotics of language model alignment. In *2024 IEEE International Symposium on Informa-*
 634 *tion Theory (ISIT)*, pp. 2027–2032. IEEE, 2024.

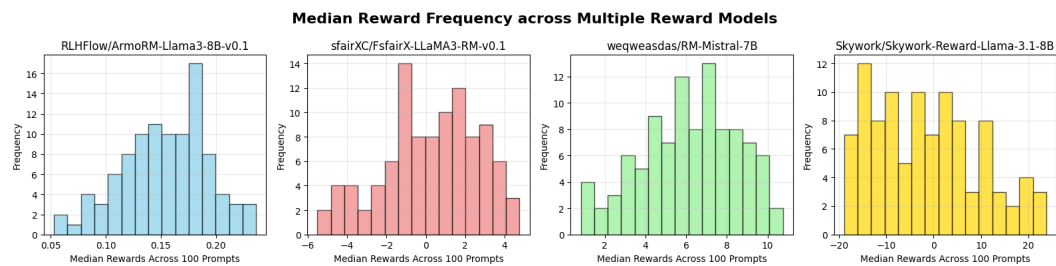
635 Shunyu Yao, Dian Yu, Jeffrey Zhao, Izhak Shafran, Tom Griffiths, Yuan Cao, and Karthik
 636 Narasimhan. Tree of thoughts: Deliberate problem solving with large language models. *Ad-*
 637 *vances in neural information processing systems*, 36:11809–11822, 2023.

638 Murong Yue, Jie Zhao, Min Zhang, Liang Du, and Ziyu Yao. Large language model cascades with
 639 mixture of thoughts representations for cost-efficient reasoning. *arXiv preprint arXiv:2310.03094*,
 640 2023.

641

648 **A DISCLOSURE OF LLM USAGE**
649650 LLMs were used to aid and polish the writing throughout the paper. In addition, LLMs were used
651 for retrieval and discovery to help write the Related Works section.
652653 **B OTHER RELATED WORKS**
654655 **Extreme Bandits.** Another related line of work is the *extreme bandit problem*, which optimizes
656 the maximum observed reward rather than cumulative reward (Streeter & Smith; Cicirello & Smith;
657 Bhatt et al., 2021). This is closely aligned with best-of- N sampling, where one selects the highest-
658 quality output among multiple candidates. However, most extreme bandit formulations assume
659 repeated rounds of play, while inference requires efficient decision-making in a single prompt. Our
660 framework adapts these insights to one-shot inference with explicit cost-quality tradeoffs.
661662 **Cascading, Routing, and Hybrid Strategies.** Beyond stopping and sampling, researchers have
663 explored *cascaded or routed inference* to reduce cost. Chen et al. (2024) escalate from cheaper
664 to larger models only when necessary, using self-testing to decide. Mohammadshahi et al. (2024)
665 learn to route prompts among multiple models, balancing cost and performance. These strategies
666 complement our focus by showing that adaptive allocation can occur across models as well as within
667 a single model’s sampling process.
668669 **C UCB PANDORA’S BOX ALGORITHM**
670671 Algorithm 2 provides the exact pseudo-code for the algorithm outlined in Section 3.
672**Algorithm 2** UCB Pandora’s Box Algorithm**Input:** Distribution family \mathcal{F} , sampling cost c .
Parameter: Confidence level parameter $\delta > 0$.

- 673 1: Initialize $S = \emptyset$ (set of observed sample values).
- 674 2: Initialize $m = -\infty$ (maximum value seen so far).
- 675 3: Initialize $\tau^+ = M_0$ (a large initial upper confidence bound for the fair cap).
- 676 4: **while** $M < \tau^+$ **do**
- 677 5: Query sample and obtain $v \sim D$.
- 678 6: $S \leftarrow S \cup \{v\}$.
- 679 7: $M \leftarrow \max\{M, v\}$.
- 680 8: Update τ^+ : Compute the UCB for the fair-cap value τ of (D, c) , based on S , \mathcal{F} , and the
681 confidence parameter δ .
- 682 9: **end while**
- 683 10: **Return:** M .

686 **D MISSING FIGURES**
687699 Figure 4: Median rewards across 960 generations for 100 prompts from the AlpacaEval dataset.
700

701 We find that the median reward across 960 generations can vary significantly across prompts.

702 **E MISSING PROOFS AND THEORETICAL RESULTS**
 703

704 **E.1 PROOF OF THEOREM 5**
 705

706 In this section, we include all missing proofs and helper lemmas needed to prove Theorem 5. The
 707 following helper lemmas will be useful.

708 **Lemma 11.** *Let D be any distribution, $c > 0$ be the cost value for each sample, and $\tau = \tau(D, c)$
 709 be the fair-cap value according to Definition 1. For every $\sigma > 0$, we have that*

710
$$\mathbb{E}_{v \sim D} [[v - (\tau + \sigma)]_+] \geq c - \sigma \cdot (1 - F(\tau)),$$

712 where F denotes the CDF of D .

714 *Proof.* Observe the following sequence of inequalities.

716
$$\begin{aligned} \mathbb{E}_{v \sim D} [[v - (\tau + \sigma)]_+] - c &= \mathbb{E}_{v \sim D} [[v - (\tau + \sigma)]_+] - \mathbb{E}_{v \sim D} [[v - \tau]_+] \\ 717 &= \mathbb{P}_{v \sim D} [v \geq \tau] \mathbb{E}_{v \sim D} [[v - \tau - \sigma]_+ - (v - \tau) | v \geq \tau] \\ 718 &\geq \mathbb{P}_{v \sim D} [v \geq \tau] \mathbb{E}_{v \sim D} [v - \tau - \sigma - (v - \tau) | v \geq \tau] \\ 719 &= (1 - F(\tau)) \cdot (-\sigma). \end{aligned}$$

721 Rearranging completes the proof. \square

722 **Lemma 12.** *Let D be any distribution, $c > 0$ be the cost value for each sample and $\tau = \tau(D, c)$ be
 723 the fair-cap value according to Definition 1. Then, for every $n \in \mathbb{N}$ and $\sigma > 0$ we have that*

725
$$\mathbb{P}_{v_{1:n-1} \sim D^{n-1}} [\max\{v_1, \dots, v_{n-1}\} \in [\tau, \tau + \sigma]] \leq F^{n-1}(\tau + \sigma) - F^{n-1}(\tau).$$

727 *Proof.* Fix $n \geq 1$ and let $M_{n-1} = \max\{v_1, \dots, v_{n-1}\}$. Observe that $\mathbb{P}[M_{n-1} \leq x] = F^{n-1}(x)$
 728 where F is the CDF of D because $v_{1:n-1}$ are iid draws. Noting that

730
$$\mathbb{P}[M_{n-1} \in [\tau, \tau + \sigma]] = \mathbb{P}[M_{n-1} \leq \tau + \sigma] - \mathbb{P}[M_{n-1} \leq \tau]$$

731 completes the proof. \square

733 **Lemma 13.** *Let D be any distribution, $c > 0$ be the cost value for each sample, and $\tau = \tau(D, c)$
 734 be the fair-cap value according to Definition 1. Then, for every $n \in \mathbb{N}$ and $\sigma > 0$, we have that*

736
$$\mathbb{E}_{v_{1:n} \sim D^n} [\Delta_n \mathbf{1}_{B_n}] \geq -\sigma(1 - F(\tau))\mathbb{P}[B_n]$$

737 where

739
$$\Delta_n := [v_n - \max\{v_{1:n-1}\}]_+ - c,$$

740 and B_n is the event that

741
$$\max\{v_{1:n-1}\} \in [\tau, \tau + \sigma].$$

742 *Proof.* (of Lemma 13) It suffices to prove the lower bound

744
$$\mathbb{E}[\Delta_n | v_{1:n-1}] \geq -\sigma(1 - F(\tau))$$

746 on the event that B_n occurs. Since v_n is independent of $v_{1:n-1}$, we have that

747
$$\mathbb{E}[\Delta_n | v_{1:n-1}] \geq \mathbb{E}[[v_n - (\tau + \sigma)]_+] - c \geq -\sigma \cdot (1 - F(\tau)),$$

749 where the last inequality follows by Lemma 11. \square

751 We are now ready to prove Theorem 5.

753 *Proof.* (of Theorem 5) Let $c > 0$ be the sampling cost and \mathcal{F} be any family of distributions that
 754 admits an anytime-valid upper confidence bound $\tau_\delta^\top(n, v_{1:n})$ with width function $\sigma_{\delta, \tau}(n)$. Fix some
 755 $D \in \mathcal{F}$ and consider the iid sequence $v_1, v_2, \dots \sim D$. Let $\tau = \tau(D, c)$ be the fair-cap value of (D, c)
 and F denote the CDF of D . For every $\delta \in (0, 1)$, let E_δ denote the event in Definition 4.

756 For $n \geq 1$, write $M_{n-1} = \max\{v_{1:n-1}\}$ and define
 757

$$758 \quad \Delta_n := [v_n - M_{n-1}]_+ - c$$

759 and
 760

$$761 \quad B_n := \{M_{n-1} \in [\tau, \tau + \sigma_{\delta, \tau}(n)]\}.$$

762 On the event E_δ , the two policies disagree only when event B_n occurs. Hence,
 763

$$764 \quad \mathbb{E}((R_W - R_U)\mathbf{1}_{E_\delta}) \leq \mathbb{E}\left[\sum_{n=1}^{\infty} -\Delta_n \mathbf{1}_{B_n} \mathbf{1}_{E_\delta}\right].$$

767 We aim to use Fubini's theorem to swap the expectation with the sum. To do so, we need to show
 768 that
 769

$$770 \quad \sum_{n=1}^{\infty} \mathbb{E}[|-\Delta_n \mathbf{1}_{B_n} \mathbf{1}_{E_\delta}|] < \infty.$$

772 To see this, note that
 773

$$774 \quad |-\Delta_n \mathbf{1}_{B_n} \mathbf{1}_{E_\delta}| \leq (c + [v_n - M_{n-1}]_+) \mathbf{1}_{B_n} \leq (c + [v_n - \tau]_+) \mathbf{1}_{B_n},$$

776 where the last inequality follows from the fact that on B_n , we have that $M_{n-1} \geq \tau$. Thus, it suffices
 777 to upper bound
 778

$$779 \quad \mathbb{E}[(c + [v_n - \tau]_+) \mathbf{1}_{B_n}].$$

780 By conditioning on M_{n-1} and using the tower law, we can write
 781

$$\begin{aligned} 782 \quad \mathbb{E}[(c + [v_n - \tau]_+) \mathbf{1}_{B_n}] &= \mathbb{E}[\mathbb{E}[(c + [v_n - \tau]_+) \mathbf{1}_{B_n} | M_{n-1}]] \\ 783 &= \mathbb{E}[\mathbb{E}[c + [v_n - \tau]_+ | M_{n-1}] \mathbf{1}_{B_n}] \\ 784 &= \mathbb{E}[c + [v_n - \tau]_+ \mathbf{1}_{B_n}] \\ 785 &= \mathbb{E}[2c \mathbf{1}_{B_n}] \\ 786 &= 2c \cdot \mathbb{P}[B_n] \\ 787 &= 2c \cdot (F^{n-1}(\tau + \sigma_{\delta, \tau}(n)) - F^{n-1}(\tau)) \\ 788 &\leq 2c \cdot F^{n-1}(\tau + \sigma_{\delta, \tau}(n)), \end{aligned}$$

790 where the third equality is by independence of v_n and M_{n-1} , the fourth equality is by definition of
 791 τ , and the sixth equality by Lemma 12. Hence,
 792

$$793 \quad \sum_{n=1}^{\infty} \mathbb{E}[|-\Delta_n \mathbf{1}_{B_n} \mathbf{1}_{E_\delta}|] \leq 2c \sum_{n=1}^{\infty} F^{n-1}(\tau + \sigma_{\delta, \tau}(n)) < \infty,$$

796 since $\sigma_{\delta, \tau}(n) \rightarrow 0$ as $n \rightarrow \infty$. Accordingly, by Fubini's theorem, we have that
 797

$$798 \quad \mathbb{E}((R_W - R_U)\mathbf{1}_{E_\delta}) \leq \sum_{n=1}^{\infty} \mathbb{E}[-\Delta_n \mathbf{1}_{B_n} \mathbf{1}_{E_\delta}].$$

801 By Lemma 13 we have that
 802

$$803 \quad \sum_{n=1}^{\infty} \mathbb{E}[-\Delta_n \mathbf{1}_{B_n} \mathbf{1}_{E_\delta}] \leq \sum_{n=1}^{\infty} \sigma_{\delta, \tau}(n)(1 - F(\tau)) \mathbb{P}[B_n].$$

806 Finally, by Lemma 12, we have that
 807

$$808 \quad \mathbb{P}[B_n] = F^{n-1}(\tau + \sigma_{\delta, \tau}(n)) - F^{n-1}(\tau),$$

809 which completes the proof. \square

810 E.2 PROOF OF COROLLARY 7
811812 In this section, we include all missing proofs and helper lemmas needed to prove Corollary 7.
813814 In order to use Theorem 5, we need to specify several things. First, Lemma 14 computes the fair cap
815 value for an Exponential distribution with parameter λ .
816817 **Lemma 14** (Fair-cap value for Exponential distribution). *Let D_λ be the exponential distribution
818 with parameter $\lambda > 0$. Then, for every $c > 0$, the fair cap value τ associated with (D, c) is $\frac{\log(\frac{1}{\lambda c})}{\lambda}$*
819820 *Proof.* For $v \sim \text{Exp}(\lambda)$, we have
821

822
$$\mathbb{E}[(v - \tau)_+] = \int_{\tau}^{\infty} (x - \tau) \lambda e^{-\lambda x} = \frac{e^{-\lambda \tau}}{\lambda}.$$

823

824 Setting this equal to $c > 0$ and solving for τ completes the proof. \square
825826 Next, we need to derive an anytime valid upper confidence bound on the fair-cap value for the
827 Exponential distribution with parameter λ . Note that an upper confidence bound on $1/\lambda$ gives an
828 upper confidence bound on τ when D_λ is an exponential distribution with parameter λ . Hence, as a
829 first step, Lemma 15 derives an anytime-valid confidence sequence for the mean of the Exponential
830 distribution.
831832 **Lemma 15** (Anytime-valid Confidence Sequence for Exponential distribution). *Fix $\lambda > 0$ and let
833 D_λ be an Exponential distribution with parameter λ . Define*

834
$$r_\delta(n) := \min\left\{\frac{1}{2}, \sqrt{\frac{6}{n} \log\left(\frac{2n(n+1)}{\delta}\right)}\right\}.$$

835

836 *Then, for every $\delta \in (0, 1)$, we have that*
837

838
$$\mathbb{P}_{v_{1:\infty} \sim D^\infty} [\forall n \geq 1 : \mu \in [\hat{\mu}_n(1 - r_\delta(n)), \hat{\mu}_n(1 + r_\delta(n))]] \geq 1 - \delta$$

839

840 *where $\mu = \frac{1}{\lambda}$ and $\hat{\mu}_n = \frac{1}{n} \sum_{i=1}^n v_i$.*
841842 *Proof.* Let $\lambda > 0$ and D_λ be an exponential distribution with parameter λ . Let v_1, v_2, \dots denote a
843 sequence of iid draws from D_λ . Define $w_i = v_i/\mu$, where $\mu = 1/\lambda$. Note that $w_i \sim \text{Exp}(1)$. Fix
844 some $n \geq 1$ and define $S_n := \sum_{i=1}^n w_i \sim \text{Gamma}(n, 1)$. Note that $\frac{\hat{\mu}_n}{\mu} = \frac{S_n}{n}$. For any $s \in (0, 1)$
845 we will show that

846
$$\mathbb{P}\left[\frac{\hat{\mu}_n}{\mu} \geq \frac{1}{1-s}\right] \leq e^{-n\psi_+(s)}$$

847

848 and

849
$$\mathbb{P}\left[\frac{\hat{\mu}_n}{\mu} \leq \frac{1}{1+s}\right] \leq e^{-n\psi_-(s)},$$

850

851 where

852
$$\psi_+(s) := \frac{s}{1-s} + \log(1-s),$$

853

854 and

855
$$\psi_-(s) := \log(1+s) - \frac{s}{1+s}.$$

856

857 Starting with the upper tail, by Markov's inequality and the MGF of the $\text{Gamma}(n, 1)$, we have that
858

859
$$\mathbb{P}[S_n \geq a] = \mathbb{P}[e^{sS_n} \geq e^{sa}] \leq \frac{\mathbb{E}[e^{sS_n}]}{e^{sa}} = (1-s)^{-n} e^{-sa}.$$

860

861 With $a = \frac{n}{1-s}$, we have that
862

863
$$\mathbb{P}\left[\frac{\hat{\mu}_n}{\mu} \geq \frac{1}{1-s}\right] = \mathbb{P}[S_n \geq a] \leq \exp\left(-n\left(\frac{s}{1-s} + \log(1-s)\right)\right) = e^{-n\psi_+(s)}.$$

864 For the lower tail, we use the fact that $x \rightarrow e^{-sx}$ is decreasing to get that
 865

$$866 \quad \mathbb{P}[S_n \leq a] = \mathbb{P}[e^{-sS_n} \geq e^{-sa}] \leq \frac{\mathbb{E}[e^{-sS_n}]}{e^{-sa}} = (1+s)^{-n}e^{sa}.$$

868 Using $a = \frac{n}{1+s}$, gives that
 869

$$870 \quad \mathbb{P}\left[\frac{\hat{\mu}_n}{\mu} \leq \frac{1}{1+s}\right] \leq e^{-n\psi_-(s)}.$$

872 Now, we show that for any $s \in (0, 1/2)$, we have that $\psi_+(s) \geq \frac{s^2}{6}$ and $\psi_-(s) \geq \frac{s^2}{6}$. For ψ_+ , define
 873 $h_+(s) = \psi_+(s) - s^2/6$. Then, note that

$$875 \quad h'_+(s) = \frac{s}{(1-s)^2} - \frac{s}{3} = s\left(\frac{1}{(1-s)^2} - \frac{1}{3}\right) \geq \frac{2s}{3} \geq 0.$$

877 Since $h_+(0) = 0$ and $h'_+ \geq 0$ we have that $h_+(s) \geq 0$. For ψ_- , we have that
 878

$$879 \quad \psi_-(s) = \log(1+s) - \frac{s}{1+s} \geq \left(s - \frac{s^2}{2}\right) - \left(s - \frac{s^2}{1+s}\right) = s^2\left(\frac{1}{1+s} - \frac{1}{2}\right) = \frac{s^2(1-s)}{2(1+s)} \geq \frac{s^2}{6},$$

881 where the first inequality is due to the fact that $\log(1+s) \geq s - \frac{s^2}{2}$ for $s \in (0, 1)$ and the last
 882 inequality uses the fact that $s \leq 1/2$. We now complete the proof by picking a summable sequence
 883 δ_n . Namely, pick $\delta_n = \frac{\delta}{n(n+1)}$ and note that $\sum_{n \geq 1} \delta_n = \delta$. At time $n \geq 1$, pick
 884

$$885 \quad r_\delta(n) := \min\left\{\frac{1}{2}, \sqrt{\frac{6}{n} \log\left(\frac{2}{\delta_n}\right)}\right\} = \min\left\{\frac{1}{2}, \sqrt{\frac{6}{n} \log\left(\frac{2n(n+1)}{\delta}\right)}\right\}.$$

888 Our previous analysis, then gives that
 889

$$890 \quad \mathbb{P}[\mu \notin [\hat{\mu}_n(1 - r_\delta(n)), \hat{\mu}_n(1 + r_\delta(n))]] \leq \delta_n.$$

891 Hence, by the union bound, we have that
 892

$$893 \quad \mathbb{P}[\exists n \geq 1 : \mu \notin [\hat{\mu}_n(1 - r_\delta(n)), \hat{\mu}_n(1 + r_\delta(n))]] \leq \sum_{n=1}^{\infty} \delta_n = \delta,$$

895 which completes the proof. \square
 896

898 Note that the anytime-valid upper confidence bound on the mean $1/\lambda$ given by Theorem 15 can be
 899 computed just from the observed rewards. Hence, it applies to *every* distribution in our distribution
 900 family \mathcal{F} . With Lemma 15 in hand, we can now prove Theorem 6, which gives an anytime-valid
 901 upper confidence bound on the fair-cap value for the family of Exponential distributions.

902 *Proof.* (of Theorem 6) Let $c > 0$ be the sampling cost and \mathcal{F} be the class of Exponential distribution
 903 with parameter $\lambda \in (0, \frac{1}{c \cdot e}]$. Fix a distribution $D_\lambda \in \mathcal{F}$. Let $\tau = \tau(D, c)$ be the fair-cap value and
 904 $\mu = \frac{1}{\lambda}$ be the mean of D_λ . Finally, let $\delta \in (0, 1)$ and consider the iid sequence $v_1, v_2, \dots \sim D_\lambda$.
 905

906 By Lemma 15, we have that
 907

$$908 \quad \mathbb{P}[\forall n \geq 1 : \mu \in [\hat{\mu}_n(1 - r_\delta(n)), \hat{\mu}_n(1 + r_\delta(n))] \geq 1 - \delta.$$

909 From Lemma 14, we know that for the exponential distribution, its cap value is a monotonic in $\frac{1}{\lambda}$.
 910 Hence, with probability $1 - \delta$, we have that

$$911 \quad \mathbb{P}\left[\forall n \geq 1 : \tau \in \left[\hat{\mu}_n(1 - r_\delta(n)) \log\left(\frac{\hat{\mu}_n(1 - r_\delta(n))}{c}\right), \hat{\mu}_n(1 + r_\delta(n)) \log\left(\frac{\hat{\mu}_n(1 + r_\delta(n))}{c}\right)\right]\right] \geq 1 - \delta.$$

914 Take $\tau_\delta^+(n, v_{1:n}) := \hat{\mu}_n(1 + r_\delta(n)) \log\left(\frac{\hat{\mu}_n(1 + r_\delta(n))}{c}\right)$. To complete the proof, it suffices to upper
 915 bound the difference
 916

$$917 \quad \hat{\mu}_n(1 + r_\delta(n)) \log\left(\frac{\hat{\mu}_n(1 + r_\delta(n))}{c}\right) - \hat{\mu}_n(1 - r_\delta(n)) \log\left(\frac{\hat{\mu}_n(1 - r_\delta(n))}{c}\right).$$

Consider the function $g(\mu) = \mu \log(\mu/c)$. Then, by the Mean Value Theorem and the fact that $g'(\mu) = 1 + \log(\frac{\mu}{c})$, we have that

$$\begin{aligned}
g(\widehat{\mu}_n(1 + r_\delta(n))) - g(\widehat{\mu}_n(1 - r_\delta(n))) &\leq \left(1 + \log\left(\frac{\widehat{\mu}_n(1 + r_\delta(n))}{c}\right)\right)(2\widehat{\mu}_n r_\delta(n)) \\
&\leq \left(1 + \log\left(\frac{\widehat{\mu}_n(1 + r_\delta(n))}{c}\right)\right)\left(\frac{2r_\delta(n)\mu}{1 - r_\delta(n)}\right) \\
&\leq \left(1 + \log\left(\frac{\mu(1 + r_\delta(n))}{c(1 - r_\delta(n))}\right)\right)\left(\frac{2r_\delta(n)\mu}{1 - r_\delta(n)}\right).
\end{aligned}$$

Recall that $r_\delta(n) \leq \frac{1}{2}$ by definition. Hence,

$$\begin{aligned}
& \left(1 + \log\left(\frac{\mu(1 + r_\delta(n))}{c(1 - r_\delta(n))}\right)\right) \left(\frac{2r_\delta(n)\mu}{1 - r_\delta(n)}\right) \leq \left(3 + \log\left(\frac{\mu}{c}\right)\right) (4r_\delta(n)\mu) \\
& = 4r_\delta(n) \cdot \tau \cdot \left(1 + \frac{3}{\log\left(\frac{\mu}{c}\right)}\right) \\
& \leq 16r_\delta(n) \cdot \tau,
\end{aligned}$$

where the last inequality follows from the assumption that $\mu \geq e \cdot c$. Hence, altogether, we can take

$$\sigma_{\delta,\tau}(n) = 16r_\delta(n) \cdot \tau.$$

which completes the proof. \square

Finally, we use Theorem 5 to bound the sub-optimality gap for UCB Pandora's Box algorithm for the family \mathcal{F} of Exponential distributions.

Proof. (of Corollary 7) Let \mathcal{F} be the class of Exponential distribution with parameter $\lambda \in (0, \frac{1}{c \cdot e}]$. Fix a distribution $D_\lambda \in \mathcal{F}$. Let $\tau = \tau(D, c)$ be the fair-cap value and let $\delta \in (0, 1)$.

Define

$$S := \sum_{n=1}^{\infty} \sigma_{\delta, \tau}(n) (1 - F_{\lambda}(\tau)) \cdot (F_{\lambda}^{n-1}(\tau + \sigma_{\delta, \tau}(n)) - F_{\lambda}^{n-1}(\tau))$$

By the Mean Value Theorem and the fact that the PDF f is monotonically decreasing, we have that for some $b \in (\tau, \tau + \sigma_{\delta, \tau}(n))$,

$$\begin{aligned} F_\lambda^{n-1}(\tau + \sigma_{\delta,\tau}(n)) - F_\lambda^{n-1}(\tau) &= \sigma_{\delta,\tau}(n) \cdot (n-1) \cdot F_\lambda^{n-2}(b) \cdot f_\lambda(b) \\ &\leq \sigma_{\delta,-}(n) \cdot (n-1) \cdot F_\lambda^{n-2}(\tau + \sigma_{\delta,-}(n)) \cdot f_\lambda(\tau). \end{aligned}$$

Plugging this back in gives that

$$\begin{aligned}
S &\leq \sum_{n=1}^{\infty} \sigma_{\delta, \tau}(n) \cdot (1 - F_{\lambda}(\tau)) \cdot \sigma_{\delta, \tau}(n) \cdot (n-1) \cdot F_{\lambda}^{n-2}(\tau + \sigma_{\delta, \tau}(n)) \cdot f(\tau) \\
&= \sum_{n=1}^{\infty} \sigma_{\delta, \tau}(n)^2 \cdot (1 - F_{\lambda}(\tau)) \cdot (n-1) \cdot F_{\lambda}^{n-2}(\tau + \sigma_{\delta, \tau}(n)) \cdot f_{\lambda}(\tau) \\
&= \sum_{n=1}^{\infty} 256 \cdot \tau^2 r_{\delta}(n)^2 \cdot e^{-\lambda \tau} \cdot (n-1) \cdot (1 - e^{-\lambda(\tau + \sigma_{\delta, \tau}(n))})^{n-2} \cdot \lambda \cdot e^{-\lambda \tau}
\end{aligned}$$

Now, observe that $r_\delta(n)^2 \leq C \frac{\log(n/\delta)}{n}$ for some universal constant C . Hence,

$$S \leq \frac{256 \cdot C \tau^2 \lambda}{e^{2\lambda\tau}} \sum_{n=1}^{\infty} \log(n/\delta) \cdot (1 - e^{-\lambda(\tau + 16\tau \cdot r_{\delta}(n))})^{n-2}.$$

It suffices to upper bound

$$\sum_{i=1}^{\infty} \log(n/\delta) \cdot (1 - e^{-\lambda(\tau + 16\tau \cdot r_{\delta}(n))})^{n-2}.$$

972 Define $A := e^{-\lambda\tau}$ and $q_n := 1 - e^{-\lambda(\tau+16\tau\cdot r_\delta(n))}$. Then, observe that

$$973 \quad 974 \quad q_n = 1 - Ae^{-16\lambda\tau\cdot r_\delta(n)}.$$

975 We want to find the smallest N such that for all $n \geq N$, we get

$$976 \quad 977 \quad 16\lambda\tau \cdot r_\delta(n) \leq \log 2.$$

978 Substituting the definition of $r_\delta(n)$ and solving for n gives that we need to set

$$979 \quad 980 \quad N \geq \Theta(\lambda^2\tau^2 \log(1/\delta)).$$

981 For this choice of N , we have that for all $n \geq N$,

$$982 \quad 983 \quad e^{-16\lambda\tau\cdot r_\delta(n)} \geq \frac{1}{2} \implies q_n \leq 1 - \frac{A}{2}.$$

985 Thus, for all $n \geq N$, we have that

$$986 \quad 987 \quad q_n^{n-2} \leq \left(1 - \frac{A}{2}\right)^{n-2}.$$

989 Now, split the infinite sum

$$990 \quad 991 \quad \sum_{n=1}^{\infty} \log(n/\delta) \cdot (1 - e^{-\lambda(\tau+16\tau\cdot r_\delta(n))})^{n-2} = \sum_{n=1}^{\infty} \log(n/\delta) \cdot q_n^{n-2} = \sum_{n < N} \log(n/\delta) \cdot q_n^{n-2} + \sum_{n > N} \log(n/\delta) \cdot q_n^{n-2}.$$

993 We can trivially bound

$$994 \quad 995 \quad \sum_{n < N} \log(n/\delta) \cdot q_n^{n-2} \leq N \log(N/\delta).$$

997 As for the second sum, we claim that

$$998 \quad 999 \quad \sum_{n > N} \log(n/\delta) \cdot q_n^{n-2} \leq \sum_{n=1}^{\infty} \log(n/\delta) \left(1 - \frac{A}{2}\right)^{n-2} \leq O\left(\frac{\log(2/\delta A)}{A}\right) = O(\lambda\tau \cdot e^{\lambda\tau} \cdot \log(1/\delta))$$

1001 To see why the second inequality is true, let $q := 1 - \frac{A}{2}$. Then,

$$1003 \quad 1004 \quad \sum_{n=1}^{\infty} \log(n/\delta) \left(1 - \frac{A}{2}\right)^{n-2} = \frac{1}{q^2} \sum_{n=1}^{\infty} \log(n/\delta) q^n.$$

1006 We will focus on bounding $\sum_n \log(n/\delta) q^n$. Define $p_n = (1 - q)q^{n-1}$. Note that p_n is the PMF of
1007 a geometric distribution p with parameter $1 - q$. Then,

$$1008 \quad 1009 \quad \sum_{n=1}^{\infty} \log(n/\delta) q^n = \frac{q}{1-q} \sum_{n \geq 1} p_n \log(n/\delta) = \frac{q}{1-q} \mathbb{E}_{n \sim p} [\log(n/\delta)].$$

1012 By Jensen's inequality and the fact that $\log(x/\delta)$ is concave, we have that

$$1013 \quad 1014 \quad \mathbb{E}_{n \sim p} [\log(n/\delta)] \leq \log(\mathbb{E}_{n \sim p} [n/\delta]) = \log\left(\frac{1}{\delta(1-q)}\right).$$

1015 Hence, we have that

$$1016 \quad 1017 \quad \sum_{n=1}^{\infty} \log(n/\delta) q^n \leq \frac{q}{1-q} \log\left(\frac{1}{\delta(1-q)}\right)$$

1019 and

$$1020 \quad 1021 \quad \frac{1}{q^2} \sum_{n=1}^{\infty} \log(n/\delta) q^n \leq \frac{1}{q(1-q)} \log\left(\frac{1}{\delta(1-q)}\right).$$

1023 Since $A \leq 1$, we have that $q \geq \frac{1}{2}$, thus,

$$1024 \quad 1025 \quad \frac{1}{q^2} \sum_{n=1}^{\infty} \log(n/\delta) q^n \leq \frac{2}{(1-q)} \log\left(\frac{1}{\delta(1-q)}\right).$$

1026 Plugging in $q = 1 - \frac{A}{2}$ completes the claim that
 1027

$$1028 \sum_{n=1}^{\infty} \log(n/\delta) \left(1 - \frac{A}{2}\right)^{n-2} \leq O\left(\frac{\log(2/\delta A)}{A}\right) = O\left(\lambda\tau \cdot e^{\lambda\tau} \cdot \log(1/\delta)\right),$$

$$1029$$

$$1030$$

1031 where the last equality follows from the definition of A . Now, returning to the original proof, we
 1032 have that
 1033

$$1034 \sum_{n=1}^{\infty} \log(n/\delta) \cdot (1 - e^{-\lambda(\tau+16\tau \cdot r_{\delta}(n))})^{n-2} \leq \tilde{O}_{\delta, \tau, \lambda}(\lambda^2 \tau^2) + \tilde{O}_{\delta}(\lambda \tau \cdot e^{\lambda \tau}).$$

$$1035$$

$$1036$$

1037 Multiplying by the outer factor gives that
 1038

$$1039 S \leq \frac{256 \cdot C \tau^2 \lambda}{e^{2\lambda\tau}} \left(\tilde{O}_{\delta, \tau, \lambda}(\lambda^2 \tau^2) + O(\lambda \tau \cdot e^{\lambda \tau}) \right)$$

$$1040$$

$$1041 = \tilde{O}_{\delta} \left(\frac{\lambda^3 \tau^4}{e^{2\lambda\tau}} + \frac{\lambda^2 \tau^3}{e^{\lambda\tau}} \right)$$

$$1042$$

$$1043 = \tilde{O}_{\delta} \left(\frac{\lambda^2 \tau^3}{e^{\lambda\tau}} \left(1 + \frac{\lambda\tau}{e^{\lambda\tau}} \right) \right)$$

$$1044$$

$$1045 = \tilde{O}_{\delta} \left(\frac{\lambda^2 \tau^3}{e^{\lambda\tau}} \right)$$

$$1046$$

$$1047 = \tilde{O}_{\delta} \left(\frac{(\lambda\tau)^3}{\lambda \cdot e^{\lambda\tau}} \right)$$

$$1048$$

$$1049 = \tilde{O}_{\delta} \left(\frac{1}{\lambda} \right)$$

$$1050$$

$$1051$$

$$1052$$

$$1053$$

1054 The third fifth equality follows from the fact that $\frac{x}{e^x} = O(1)$ and $\frac{x^4}{e^x} = O(1)$ respectively. This
 1055 completes the proof. \square

1057 F ADDITIONAL EXPERIMENTAL RESULTS

$$1058$$

1059 This appendix provides comprehensive experimental results across all datasets, language models,
 1060 and reward models. While Section 5 focused on representative examples, here we present the
 1061 complete evaluation demonstrating the consistency and robustness of our adaptive approach. **All empirical**
 1062 **results in this section fix $\alpha = 0.99$. We study the impact of other choices for α in Appendix**
 1063 **F.5.**
 1064

1065

1066 F.1 EXPERIMENT 1: PROFIT PERFORMANCE ACROSS ALL CONFIGURATIONS

$$1067$$

1068 We evaluate how consistently our adaptive algorithm matches optimal non-adaptive performance
 1069 across diverse settings. The profit performance ratio is defined as:

$$1070 \text{Profit Performance Ratio} = \frac{\text{Profit of Adaptive Best-of-N}}{\text{Profit of Best Non-adaptive Best-of-N}}$$

$$1071$$

$$1072$$

1073 where profit equals utility minus total generation cost. A ratio near 1.0 indicates the adaptive algo-
 1074 rithm matches the best possible non-adaptive strategy without requiring hyperparameter tuning.

1075 The results, shown in Figure 5 for the AlpacaFarm and HH-RLHF datasets with RM-Mistral-7B and
 1076 FsfairX-LLaMA3-RM-v0.1, confirm the adaptive algorithm’s strength.
 1077

1078 The adaptive algorithm outperforms most of the time even the best-tuned generator dependent non-
 1079 adaptive strategy. This implies that its dynamic behavior is more profitable than any fixed, one-size-
 fits-all approach.

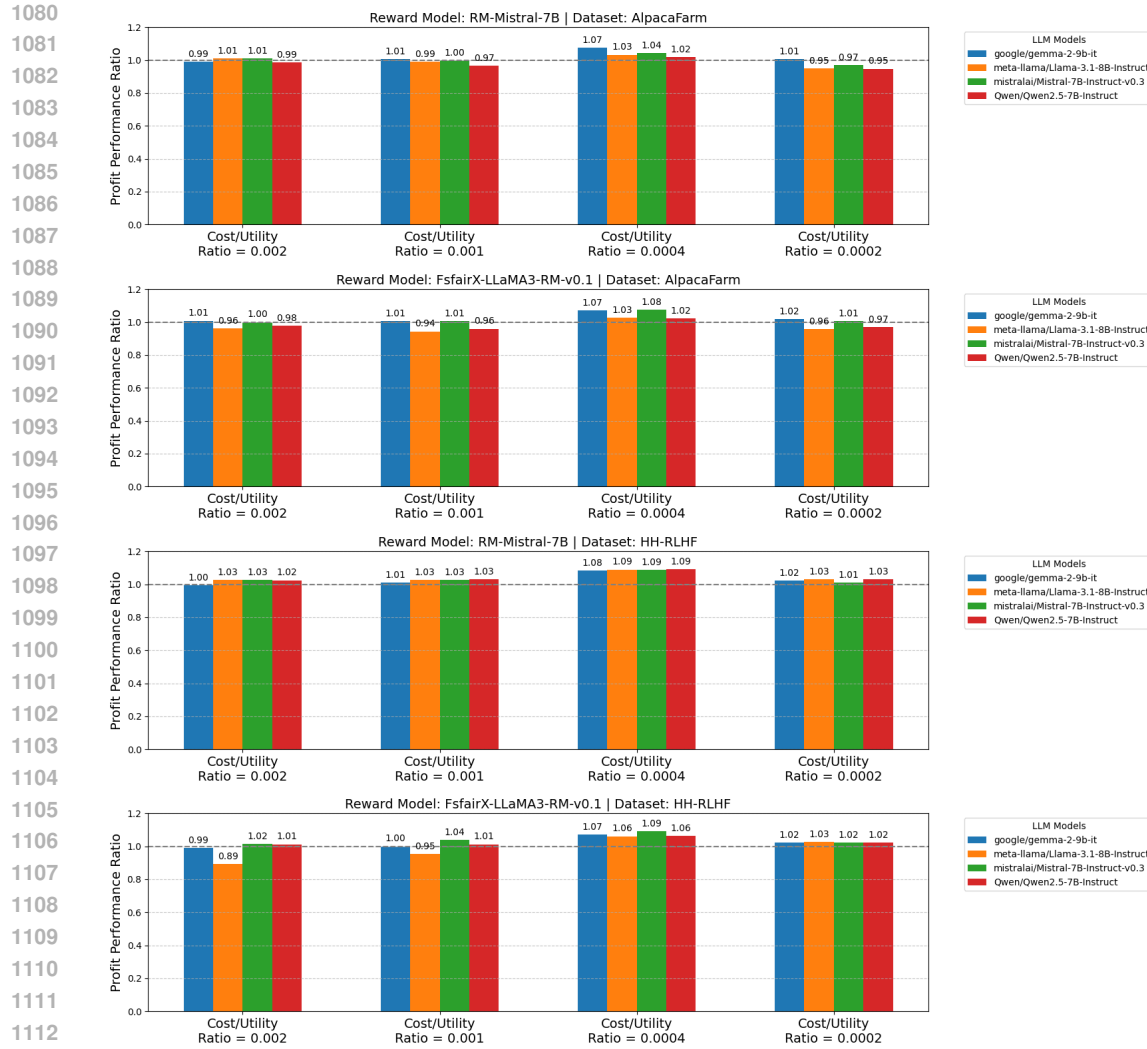


Figure 5: Profit performance ratios for four LLM generators across varying cost/utility ratios. Each panel represents a different dataset-reward model combination, with four cost/utility scenarios per panel. Higher ratios indicate better profit efficiency relative to best non-adaptive algorithm.

F.2 EXPERIMENT 2: WIN RATE ANALYSIS ACROSS CONFIGURATIONS

We compare head-to-head performance when adaptive and non-adaptive algorithms use identical computation budgets.

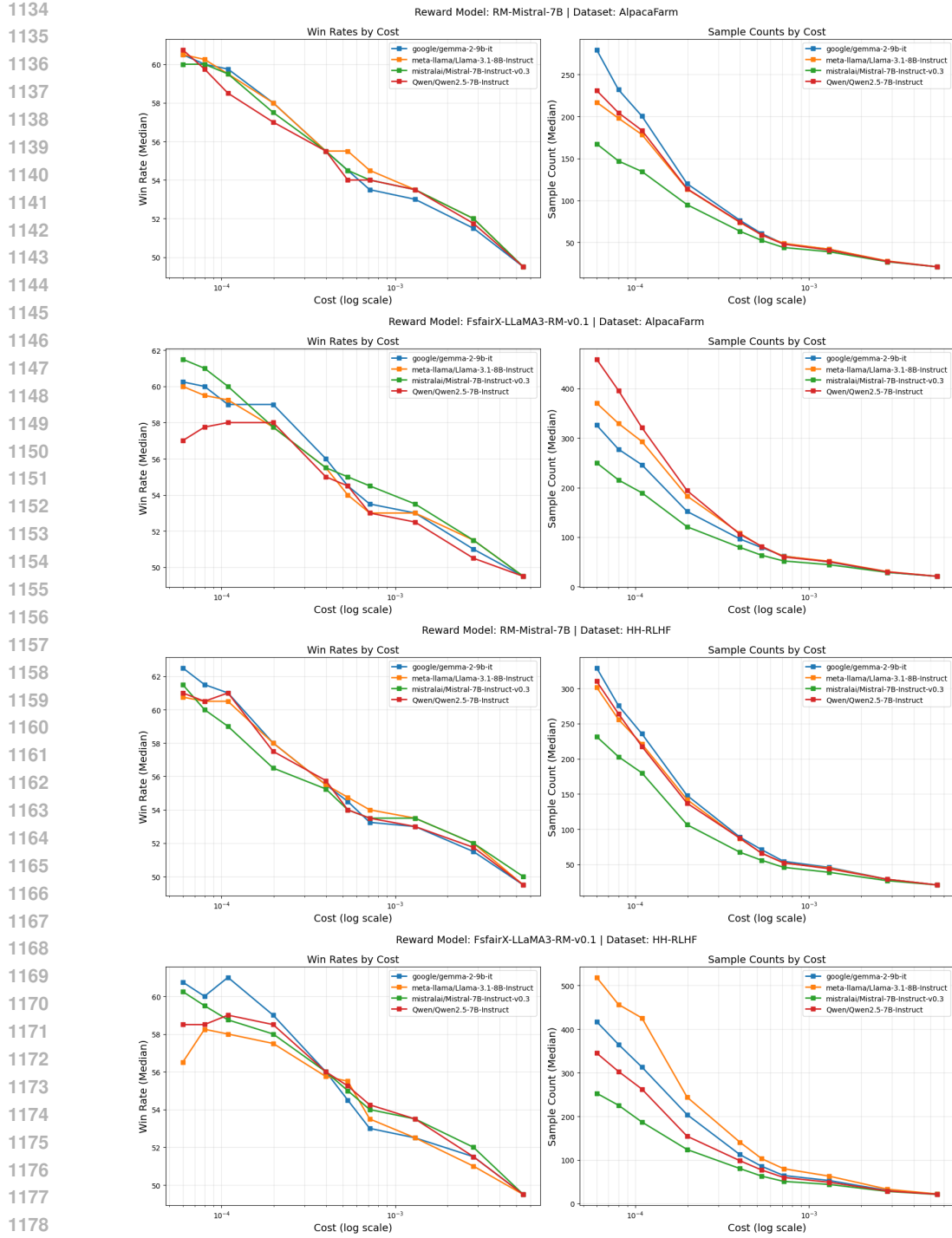


Figure 6: Performance evaluation of adaptive versus non-adaptive generation under matched computational budgets. Each row corresponds to a unique reward model-dataset configuration. Left panels present win rates computed from 100 sample permutations where adaptive algorithms compete against non-adaptive baselines. Right panels show mean sample counts (identical for both strategies due to budget matching) averaged over the same 100 permutations. Both metrics are plotted against cost (log scale, 10^{-5} to 10^{-2}) and represent median values across all evaluation prompts.

Figure 6 reveals consistent patterns across all settings:

1188 • **Budget scaling:** The adaptive algorithm’s advantage grows with the available budget. Its
 1189 win rate increases from around 50% (at chance) with minimal resources to over 54% when
 1190 the budget exceeds 100 samples.
 1191
 1192
 1193
 1194
 1195
 1196
 1197
 1198
 1199
 1200
 1201 • **Model consistency:** The win rate trends are remarkably consistent across different models.
 1202 This demonstrates that the algorithm’s effectiveness is not tied to a specific model.
 1203
 1204
 1205
 1206
 1207
 1208
 1209
 1210
 1211
 1212 • **Dataset effects:** Similarly, the performance curves hold steady across different datasets,
 1213 proving the algorithm is robust to variations in input data and prompt styles.
 1214
 1215
 1216
 1217
 1218
 1219
 1220 This consistent advantage across diverse models, datasets, and budgets validates our central hypothesis:
 1221 the adaptive algorithm succeeds by exploiting the unique reward distribution of each prompt,
 1222 rather than relying on a specific setup.
 1223
 1224
 1225
 1226
 1227
 1228
 1229
 1230
 1231
 1232
 1233

1234 F.3 EXPERIMENT 3: EFFICIENCY GAINS AT TARGET QUALITY LEVELS

1235
 1236
 1237
 1238
 1239
 1240 This experiment quantifies the computational efficiency of our adaptive algorithm. We measure how
 1241 many fewer samples it needs than a non-adaptive approach to reach the same quality, defined by the
 acceptance rate.

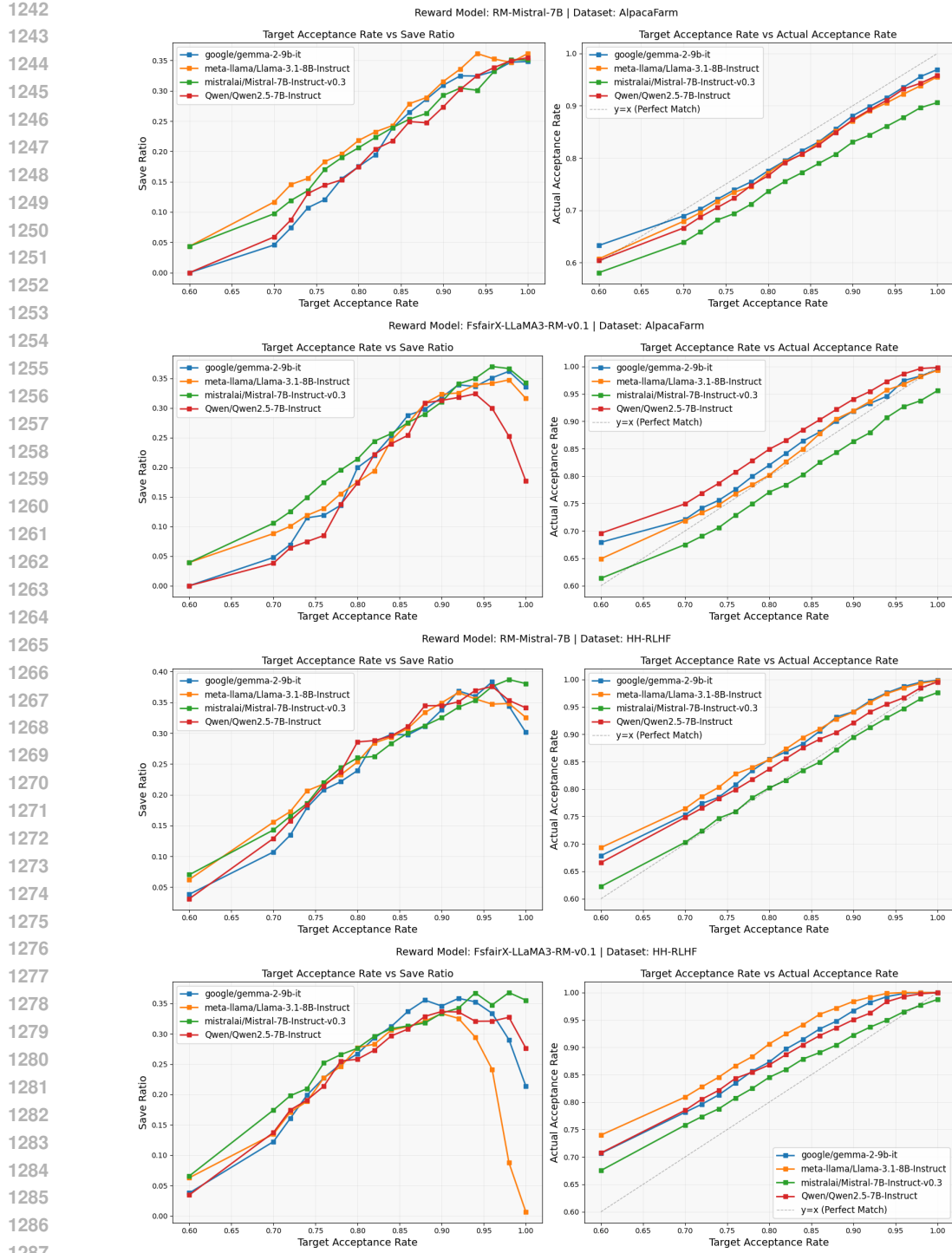


Figure 7: Computational savings from adaptive generation while maintaining acceptance rate equivalence. Each row presents a unique reward model-dataset pairing. Left panels quantify the save ratio—the fraction of samples eliminated by adaptive algorithms compared to non-adaptive methods when both achieve identical average acceptance rates. Specifically, for each target acceptance rate, the adaptive algorithm yields an actual acceptance rate, and the non-adaptive sample count is calibrated to match this actual rate. Right panels show the relationship between target and actual acceptance rates for the adaptive algorithm, illustrating calibration behavior. Save ratios are averaged over 100 generation stream permutations, with all metrics indexed by target acceptance rate (0.6–1.0) and aggregated via median across 100 test prompts.

1296

Figure 7 demonstrates two critical findings:

1297

1298

1299

1300

1301

Right panels (Target vs Achieved Rates): The adaptive algorithm effectively follows the desired quality targets. While a small gap exists between the target and achieved acceptance rates, the graphs confirm that our algorithm reliably adjusts its behavior to closely approximate the specified quality level across all configurations.

1302

1303

Left panels (Compute Savings): The algorithm delivers significant efficiency gains, with savings that peak when targeting high levels of quality. The trend is as follows:

1304

1305

1306

1307

1308

1309

1310

- Savings increase from 10% at a moderate quality target (0.70 acceptance rate) to a peak of $\sim 30\%$ for near-optimal targets (0.90+ acceptance rate).
- However, savings decrease as the target approaches 100%. This is because the extreme quality requirement forces the adaptive algorithm to use its maximum sample budget, causing its behavior to converge with the non-adaptive baseline. Importantly, even in this scenario, it never performs worse.

1311

1312

1313

1314

This peak in savings at high (but not perfect) quality levels demonstrates the algorithm’s core strength: its ability to recognize when a near-optimal response has been found and stop generation early. In contrast, non-adaptive methods must always continue sampling to maintain the same quality guarantee.

1315

1316

Efficiency gains increase monotonically with target quality:

1317

1318

1319

1320

1321

1322

1323

1324

1325

- Roughly 10% savings at 0.70 acceptance rate (moderate quality)
- Roughly 20% savings at 0.80 acceptance rate (good quality)
- Roughly 30% savings at 0.90+ acceptance rate (near-optimal quality)
- When 100% acceptance rate is targeted, our experimental setup suffers from maximum sample size leading that adaptive algorithm becomes closer to non-adaptive one. This explains decrease on save ratio as we get close to 100% target acceptance rate though it never performs worse than non-adaptive algorithm with same computation budget.

1326

1327

1328

The increasing savings at higher quality levels reflect the adaptive algorithm’s ability to recognize when it has likely found a near-optimal response, while non-adaptive methods must continue sampling to maintain guarantees.

1329

1330

F.4 CROSS-DATASET AND CROSS-MODEL INSIGHTS

1331

1332

A cross-experimental analysis of our results reveals three consistent and noteworthy findings:

1333

1334

1335

1336

1337

1338

1339

1340

1341

1342

1343

1344

1345

1346

- **Robustness Across Configurations:** The performance metrics and advantages of the adaptive algorithm remained consistent across all 1,600 unique generation profiles. This demonstrates that the approach generalizes effectively and is not over-fit to specific model-dataset pairings.
- **Positive Scaling with Budget:** The superiority of the prompt-adaptive algorithm becomes more pronounced as the number of candidate generations increases, indicating that its advantages scale positively with a larger computational budget.
- **Reward Model Independence:** The performance trends were congruent for both the RM-Mistral-7B and FsfairX-LLaMA3-RM-v0.1 reward models. This suggests that the benefits of the adaptive strategy are independent of the specific reward function employed.

1347

1348

1349

F.5 IMPACT OF α

In this section, we present empirical performance of UCB Pandora’s Box (Algorithm 1) for gold-standard quantiles $\alpha \in \{0.50, 0.75\}$. From Figures 8 and 9, we find that Algorithm 1 is robust to the choice of α and obtains similar empirical results to when $\alpha = 0.99$. Similar results are observed for the HH-RLHF dataset and FsfairX-LLaMA3 reward model.

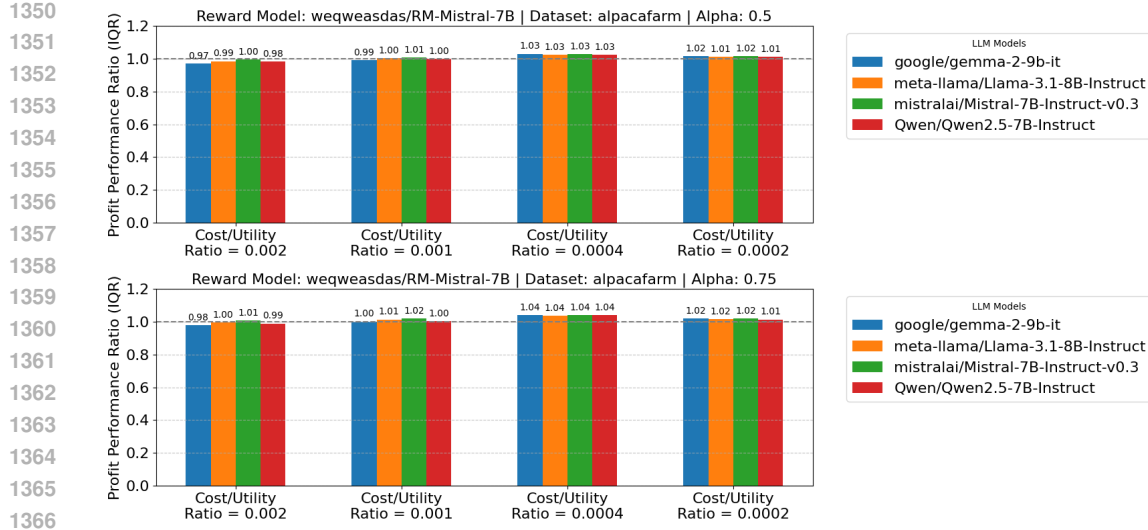


Figure 8: PPRs of UCB Pandora’s Box (Algorithm 1) for gold-standard quantiles $\alpha \in \{0.50, 0.75\}$ on the AlpacaFarm dataset and RM-Mistral-7B reward model.

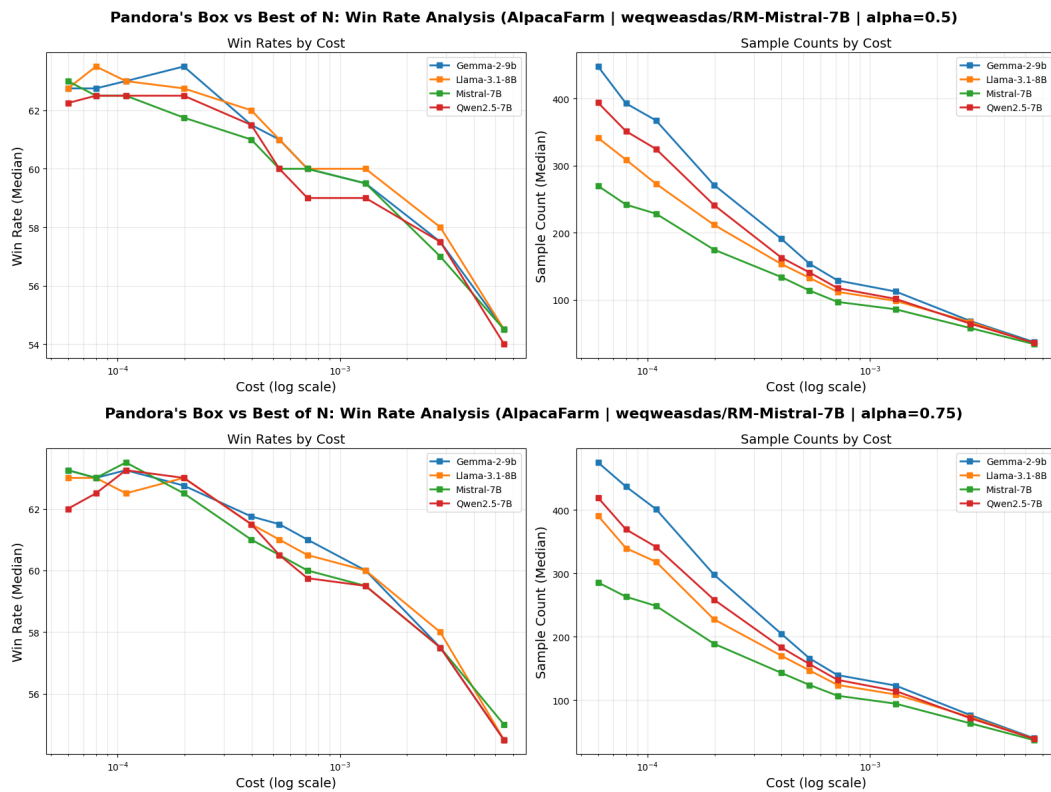


Figure 9: Win rates and sample counts of UCB Pandora’s Box (Algorithm 1) for $\alpha \in \{0.50, 0.75\}$ on the AlpacaFarm dataset and RM-Mistral-7B reward model.

F.6 QQ-PLOTS

In this section, we empirically corroborate our choice to use the Exponential distribution to fit the right-tail of the exponentiated rewards. Figure 10 presents QQ-plots of the exponentiated rewards

against a (shifted) exponential distribution on four prompts from the AlpacaFarm dataset for the RM-Mistral-7B reward model. The almost linear nature of the blue dots indicate that the Exponential distribution generally fits the right-tail of the exponentiated rewards well. Similar results are observed for other prompts in the AlpacaFarm and HH-RLHF datasets as well as the FsfairX-LLaMA3 reward model.

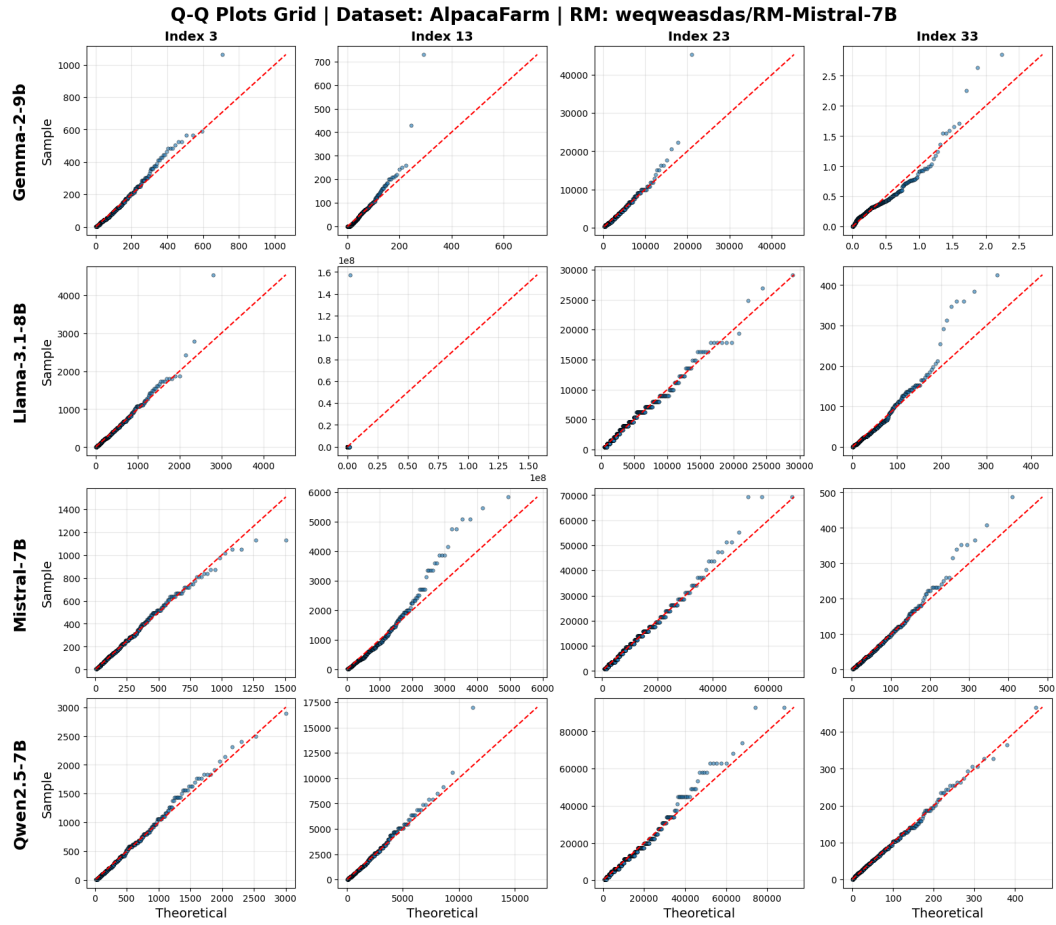


Figure 10: QQ-plots of the right-tail of the exponentiated rewards from the RM-Mistral-7B reward model against a shifted Exponential distribution for four prompts from the AlpacaFarm dataset.

F.7 COMPARISON WITH NAIVE BASELINE

In this section, we compare our method against a naive adaptive baseline which stops sampling once the maximum reward seen so far has not changed for 5 steps. Figure 11 presents the median profit of Algorithm 1, the naive adaptive baseline, and the profit of the non-adaptive BoN (for various N values) across prompts from the AlpacaFarm dataset using the the RM-Mistral-7B reward model. We find that across a wide range of cost values and LLMs, the naive baseline obtains smaller profit than our adaptive method. Moreover, this difference in profit between Algorithm 1 and the naive baseline increases as the cost/utility ratio decreases. Similar results are observed for the HH-RLHF dataset and FsfairX-LLaMA3 reward model.

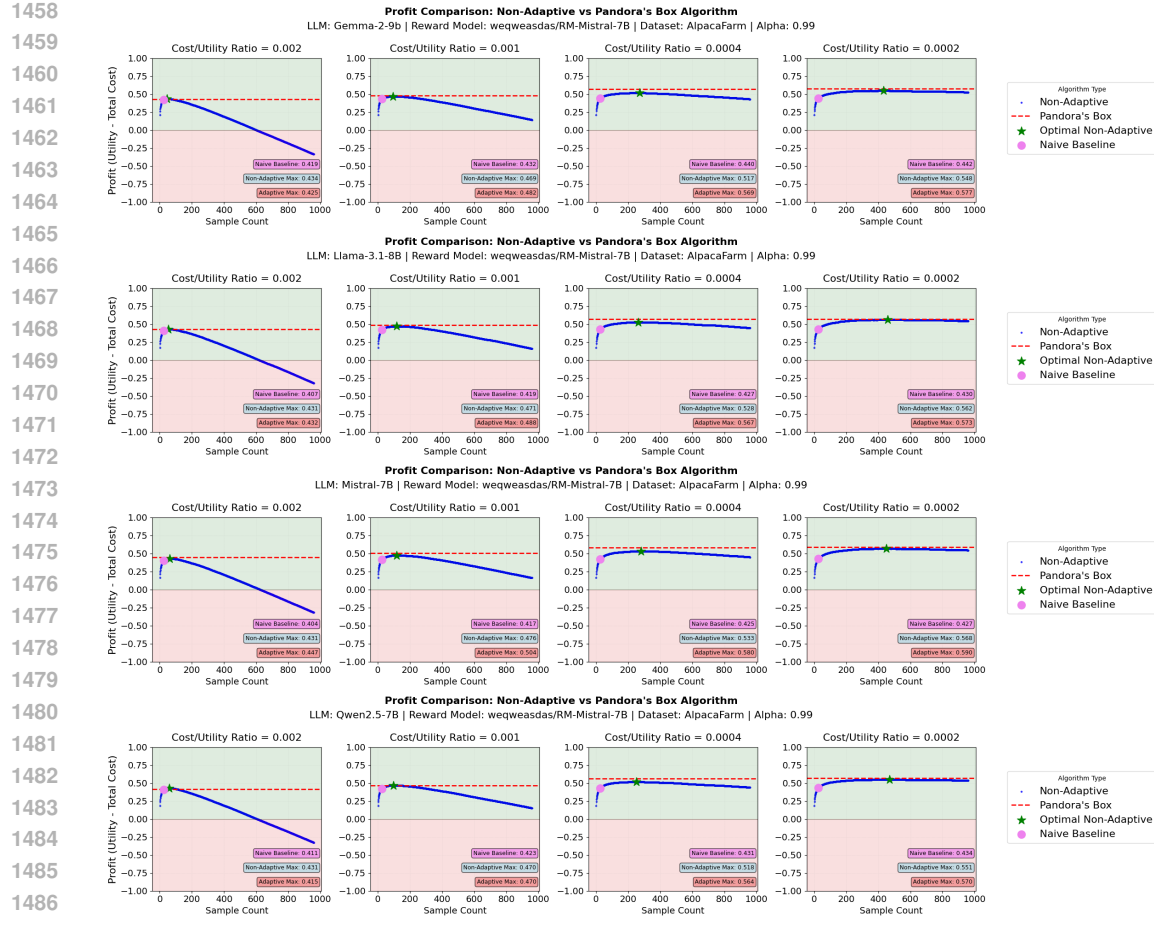


Figure 11: Median profit (over prompts from the AlpacaFarm dataset) of UCB Pandora's Box (Algorithm 1), the naive baseline, and the non-adaptive BoN (at various N values) for cost/utility ratios $c \in \{0.002, 0.001, 0.0004, 0.0002\}$.